Physics and Chemistry of the Earth 139 (2025) 103909

Contents lists available at ScienceDirect

Physics and Chemistry of the Earth

journal homepage: www.elsevier.com/locate/pce

Projection of precipitation variability over the highlands of Yemen by statistical down-scaling for the period 2026–2100

Ali H. AL-Falahi [a,*], Solomon H. Gebrechorkos [b], Naeem Saddique [c], Uwe Spank [a], Christian Bernhofer [a]

[a] Meteorology, Institute of Hydrology and Meteorology, Technische Universität Dresden, Pienner Str. 23, D-01737, Tharandt, Germany
[b] School of Geography and Environmental Science University of Southampton, SO17 1BJ, Southampton, United Kingdom
[c] Department of Irrigation and Drainage, University of Agriculture, 38040, Faisalabad, Pakistan

ARTICLE INFO

Keywords:
Statistical down-scaling model
Precipitations
Climate change impact
Water management
Highland region of Yemen

ABSTRACT

Climate change significantly affects the management of environmental resources, particularly through changes in the amount and variability of local climate variables, such as precipitation. However, current projections from Global Climate Models (GCMs) are not directly applicable to local-scale impact modeling due to their coarse spatial resolution and inherent biases. To address this challenge, the Statistical Down-Scaling Model (SDSM) is employed to downscale daily precipitation, a crucial input for impact assessment models. This study focuses on the highlands of Yemen, a region highly vulnerable to climate change and precipitation variability. Due to limited and incomplete local climate data, we utilized the best available precipitation datasets, including the Climate Hazards Group Infra-Red Precipitation with Station data (CHIRPS), to fill in missing station data. Historical and future predictors derived from the National Center for Environmental Prediction (NCEP) reanalysis and the Canadian Earth System Model Phase 2 (CanESM2) were used to generate future precipitation scenarios, which were compared with the ensemble means from the Coupled Model Intercomparison Project Phase 5 (CMIP5) and the Coupled Model Intercomparison Project Phase 6 (CMIP6). We also used the Shared Socioeconomic Pathways (SSPs) scenarios, specifically SSP126 and SSP585, to evaluate potential future changes in precipitation. Results indicate a projected increase in seasonal precipitation during the 2030s (2026–2050), 2060s (2051–2075), and 2090s (2076–2100). The western highlands, including Al Mahwit, Rymah, and parts of Sana'a governorate, are expected to experience precipitation increases of up to 55 %. Under RCP2.6, the short rainy season (March–May) is projected to increase up to 14 %, while under RCP8.5, this increase could reach 24 %. The long rainy season (June–August) is expected to increase by 6 % under RCP2.6 and 27 % under RCP8.5. The dry season (December–February) could see increases of 18 % under RCP2.6 and 46 % under RCP8.5, while the autumn season (September–November) may experience a substantial rise of 61 %–101 %. At the annual timescale, precipitation is projected to increase up to 34 % higher than the baseline period (1991–2020) across the region. These projections indicate that the highlands of Yemen will experience wetter conditions in the 21st century. The findings provide valuable insights for developing adaptation strategies for water and environmental resource management, considering the potential future impacts of climate change in the region.

1. Introduction

Over the last half-century, the global climate has warmed primarily due to increased concentrations of greenhouse gases caused by human activity (Rama et al., 2022). Continued emissions of greenhouse gases at or above current rates will lead to further warming during the 21st century, which in turn affects the hydrological cycle and rainfall timing in many regions. According to global projections, changes in precipitation averages in a warmer world will exhibit substantial spatial variation. The frequency and intensity of heavy precipitation will also change as a result of climate change (Poschlod, 2021). Characteristics and frequency (probability) of dry and wet spells in many regions are expected to change in response to climate change impact (Ye, 2018). Some regions will experience a decrease in rainfall average rates and

* Corresponding author.
E-mail address: ali.al-falahi@tu-dresden.de (A.H. AL-Falahi).

https://doi.org/10.1016/j.pce.2025.103909
Received 1 October 2024; Received in revised form 25 February 2025; Accepted 19 March 2025
Available online 22 March 2025

perturbation of rainfall durations, while some other regions are projected to experience an increase and spatial variation of rainfall, and yet others will not experience significant changes at all (IPCC, 2014). Further, there is a chance that extreme precipitation events will become more intense and frequent over most mid-latitude land masses and wet tropical regions, where water will continue to warm and acidify and the global mean water level will continue to rise (Zeleňáková et al., 2022).

Across the Middle East and North Africa (MENA) region, there is increasing confidence in the projected patterns of warming and sea-level rise, but there is less confidence in the changes in regional patterns of rainfall and the incidence of extreme rainfall events (Ozturk et al., 2021). In Yemen, for instance, considerable uncertainty in climate model projections does exist, especially for local precipitation (Wilby and Yu, 2013). Yemen is an arid sub-tropical country where temperature depends primarily on elevation and is influenced by distance from the sea in the coastal areas. Mean temperatures of Yemen range from 15 °C in winter to 25 °C in summer and from 22.5 °C in winter up to 35 °C during summer in the coastal lowlands. Rainfall patterns differ in the highlands and coastal areas with relatively little rainfall received in the center of the country (Ward and Wan, 2020). The annual frequency of rainy days increases with elevation, exhibiting a significant decrease in the wet days from west to east (Hadden, 2012). Rainfall in the highlands follows two distinct rainy seasons: the Saif (March–May) and the Kharif (June–August), while the coastal areas receive 80 % of the annual rainfall during winter months. The Kharif rainfall is governed by mechanisms of the Inter-Tropical Convergence Zone, which typically occur in short events, while, the Saif rains are governed by the north-west trade winds entering the Red Sea Convergence Zone (GFDDR, 2011).

Further, Yemen is a vulnerable region to climate change and climate variability (Alderwish and Al-Eryani, 1999; Almas and Scholz, 2006). Agriculture and water resources are the most vulnerable sectors to climate change and are extremely affected by changes in temperature increase and precipitation variability (Haidera and Noaman, 2010; Rahman et al., 2012). According to projections by Global Climate Models (GCMs) and the few available local studies, climate extreme events and multiple natural hazards such as intense rainfall events and floods (Al-Jibly, 2008; EPA, 2013) are likely to increase over large territories of Yemen. These events may also contribute to declines in real household incomes and exacerbate food insecurity (Al-Riffai et al., 2013; Breisinger et al., 2011), especially in the high-populated zones. At least, one natural disaster (severe droughts from 2007 to 2009) with adverse impact on the livestock, agriculture, and agricultural lands has been reported every year over the last twenty years in Yemen as a result of climate variability (Miyan, 2015).

Generally, GCMs provide reliable information on the variability and changes in large-scale climate. The models can provide high-quality climate information on global, continental, and large regional scales with greatly varying potential for floods and droughts (IPCC, 2013; IPCC, 2014). The GCMs are skilled at replicating past and current climates as well as accurately reproducing observed temporal warming trends and sea ice dynamics (Rosenblum and Eisenman, 2017). The climate models project possible future climate shifts under the conditions of specific scenarios (Varotsos et al., 2021). Nevertheless, the horizontal resolution of GCMs (>100 km) limits the possibility of addressing smaller scales ranging from regional to local scale and cannot accurately capture the local forcing factors such as complex topography and land-surface characteristics (Chenet et al., 2021). Moreover, the GCMs face large biases and uncertainties in representing the current and future climate (Sachindra et al., 2012) and the uncertainties increase at the local scale (Joetzjer et al., 2013; Knutti and Sedlacek, 2012; Lutz et al., 2013), which requires an intensive evaluating of GCMs output before being utilized.

To improve the resolution of GCMs, down-scaling techniques, such as dynamical and statistical, have been developed to obtain high-resolution climate or climate change information from relatively coarse-resolution global climate models. Dynamical and statistical down-scaling is the most widely applied technique to transfer changes in large-scale climate variables (predictors) to regional or local scale meteorological variables (predictands) (Trzaska and Schnarr, 2014a; Zhang et al., 2019). The dynamical down-scaling is applied for various temporal scales and employs a high-resolution model (a regional climate model (RCM)) driven by GCM boundary conditions to derive smaller-scale information. One distinct advantage of RCM application is its higher horizontal resolution, facilitating a more accurate representation of vital climate phenomena including clouds and terrestrial surface processes/features (e.g., topography), especially when RCM provides cloud-permitting resolutions to avoid the cumulus parameterization issues (Gutowski et al., 2020).

Most of the RCMs have a horizontal resolution between 0.11° and 0.50° (Giorgi, 2019) driven by the GCM results, which assumes that the large-scale characteristics of the GCM results or analyses would be, at least, produced by these applications and finer information at different scales will be added (Gnitou et al., 2022). However, the applicability of the dynamical downscaling, even with its higher spatial resolution when compared with the resolution provided by the GCMs is still limited in the impact assessment studies at a local scale due to resource requirements, complexity of the models, biases and sensitivity of the models to the boundary condition of GCMs (Gebrechorkos et al., 2019a,b; Hamlet et al., 2010).

Conversely, down-scaling based on statistical models requires less processing and computational expenses, which makes it more effective, simple, and faster than dynamical down-scaling (Gebrechorkos et al., 2019a,b). The statistical down-scaling (SD) is used to transform the outputs from GCMs to the local scale by establishing a statistical link between the local-scale meteorological series (predictand) and large-scale atmospheric variables (predictors) (Fan et al., 2021). It is commonly used to provide information for the assessment of climate change impacts. SD aims to provide a finer grain of detail and to mitigate systematic biases using the output from large-scale dynamical climate models and observation-based data products, which is recognized as providing added value (Lanzante et al., 2017). In the face of climate change, the relationship used to train the method during the historical period is unchanged in the future is one of the key assumptions of SD (Trzaska and Schnarr, 2014). The implicit assumption in all empirical-statistical downscaling (ESD) methods is that the transfer relationship, derived from historical data, is valid in a future period during which fundamental aspects of the climate system may have changed (Lanzante et al., 2017).

In this study, we developed fine-scale climate projections for the highland region of Yemen, namely Sana'a, Amran, Al Mahwit, Thamar, and Raymah governorates by application of the Statistical Down-Scaling Model (SDSM), a hybrid of transfer function and stochastic weather generator. The primary objective of this research is to overcome the limitations of previous climate studies in Yemen (Alderwish and Al-Eryani, 1999; Almas and Scholz, 2006), which relied on coarse-resolution outputs from Global Climate Models (GCMs). By generating fine-scale, station-level projections, we aim to provide actionable insights for local-scale applications, such as hydrological management and climate adaptation planning.

A few studies (Al-Jibly, 2008; EPA, 2013) on climate change impact have been done in some areas within the highland region of Yemen employing GCMs coarse projections (>100 km). However, these studies were constrained by data scarcity and a lack of high-temporal-resolution data, such as daily time series, which are critical for localized projections. Furthermore, their coarse resolution posed challenges in capturing the unique climatic variations at smaller spatial scales, such as watersheds or districts. The current study addresses these limitations by utilizing robust station-level data to establish a statistical connection between local predictands (e.g., precipitation data) and predictors derived from GCMs (AL-Falahi et al., 2020).

To address the gaps identified in earlier research (Alderwish and Al-Eryani, 1999; Almas and Scholz, 2006) our study employs a

downscaling approach to generate improved and dependable estimates at finer spatial resolutions. This is achieved by integrating high-resolution gridded data (CHIRPS) with GCM outputs from CMIP5 and CMIP6 to evaluate and refine the projections. The SDSM methodology is designed to enhance the accuracy and reliability of climate projections by bridging the gap between coarse GCM outputs and the fine spatial resolution required for local decision-making.

To the best of our knowledge, this is the first study to project the potential impact of climate change over the highland region of Yemen using a combination of ground observations and high-resolution gridded data, supplemented by CMIP5 and CMIP6 datasets. This novel approach provides robust climate projections with finer resolution, addressing critical challenges such as data scarcity and coarse model outputs. Our projections are particularly valuable for researchers and policymakers working on water resource management, hydrology, and climate adaptation in the region. By applying the SDSM, our hypothesis suggests that the generated projections are more objective for local-level use, especially for hydrological and basin unit management.

In summary, this study fills a significant knowledge gap in climate change research for Yemen and provides a framework for addressing similar challenges in other data-scarce regions. It examines observed and projected climate trends in Yemen, considering the limitations posed by data scarcity and evaluating methodologies to enhance climate projections in such conditions. Furthermore, the study explores how these findings can inform localized adaptation and mitigation strategies, ensuring that interventions are tailored to Yemen's specific vulnerabilities. Ultimately, the insights gained from this research have broader implications, offering a methodological approach that can be applied to other regions facing similar climate and data challenges.

1.1. The study area

The study is conducted in the highland region of Yemen. The region is located in the northwest of Yemen at an altitude ranging from 150 to 3666 m above sea level (Fig. 1).

The region occupies an area of around 39,434 km^2 and is characterized by high population density representing 53 % of the Yemeni population (AL-Falahi et al., 2020; Fischer et al., 2010; Varisco, 2018). The region consists of five governorates: Sana'a, Amran, Al Mahwit, Raymah, and Thamar. However, the exact boundary of the region can differ in some references (Al-Hawshabi and El-Naggar, 2015; Bosworth et al., 2005; van der Gun and Ahmed, 1995; Moore, 2011), where two or three governorates may be included, namely Ibb, Hajjah, and Saadah, which are excluded in this study because of the absence of ground data at the beginning stage when we evaluated gridded products against ground data. Temperature is moderate to cold throughout the year in the region and rainfall occurs in two seasons Al Saif and Al Kharif. Short and long rain seasons are March–May (MAM) and from June to August (JJA), respectively (Ruijs et al., 2011). The annual rainfall average is around 350 mm in the west and about 200 mm yr $^{-1}$ in the east, particularly from Sana'a city towards Khawlan Al Teal districts and Marib governorate (Buhairi, 2010; Wiebelt et al., 2011). The most important rain time for rainfed agriculture is June–August, while the driest season is in winter from December through February (DJF).

Agriculture is the main activity of local people and several crops and productive trees such as qat, grapes, wheat, sorghum, corn, coffee, and barley are cultivated in the area. Rainfed agriculture and the old terrace agricultural system are the unique features of the region in comparison to the other agricultural regions in the Arabian Peninsula. The agricultural system in the highland of Yemen is one of the oldest and most sophisticated agricultural regimes in the world (Muharram and Alsharjabi, 2019; Pietsch and Mabit, 2012; Varisco, 1991). Over the last

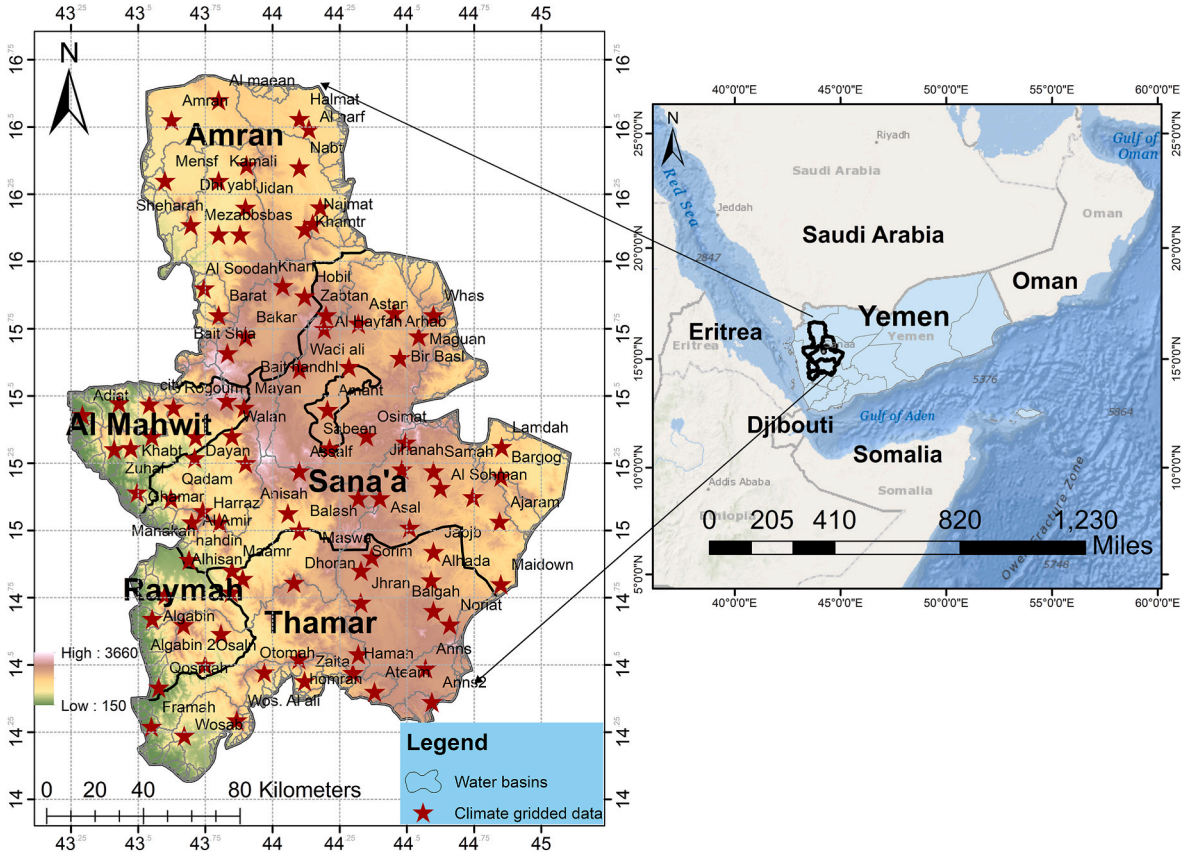

Fig. 1. Map of the highland region displaying location and name of climate employed stations.

40 years, the region has experienced several climate and climate-related hazards such as droughts, floods, soil salinity, landslides, and sandstorms. At least three to four sand storms were registered during 2013–2020, a phenomenon that is considered unusual to occur in this complex-mountainous territory (AL-Falahi et al., 2020).

The selection of this region is primarily based on its climatic and topographic homogeneity, as well as its relatively high seasonal rainfall compared to the other regions of Yemen. Moreover, the availability of daily and monthly precipitation station data, which were essential for evaluating and verifying gridded data in the initial analysis, made this region a preferred choice (AL-Falahi et al., 2020).

2. Material and methods

The model relies on four primary datasets as input; ground-based observations supplemented with Climate Hazards Group InfraRed Precipitation with Station data (CHIRPS); Reanalysis data of the National Center for Environmental Prediction/the National Center for Atmospheric Research (NCEP/NCAR1); Predictors from the Second-Generation Canadian Earth System Model (CanESM2) and the Canadian Earth System Model Version 5 (CanESM5); and Representative Concentration Pathways (RCP2.6, RCP8.5) of the Coupled Model Intercomparison Project Phase 5 (CMIP5). Additionally, ensemble means of GCMs under CMIP5 and CMIP6 were utilized during the validation period and for comparison with historical data and projections of SDSM.

2.1. Datasets

2.1.1. High-resolution gridded precipitation

Climate data and long-time measurements of climate variables (precipitation) are scarce in Yemen. There are few numbers of meteorological stations with short time records and data gap is often encountered due to drawbacks and difficulties such as political and security unstable conditions of the country, limited budget available to operate and maintain remote ground stations, and poor documentation of ground data by the collecting agencies. Moreover, most of the data collected are available at a monthly timescale, while the daily measurements are very short and not easily accessible to the public and researchers. In addition to the available daily and monthly ground data, this study incorporates CHIRPS gridded daily data as a supplementary dataset. This data helps to fill gaps in ground measurements for the reference period from 1991 to 2020.

According to Wilby and Dawson (2013), high spatial and temporal resolution products (e.g. remote sensing precipitation products) can be used for statistical down-scaling in data-sparse regions. Across the highland region of Yemen, CHIRPS along with highly advanced and latest applied reanalysis and satellite products (TRMM 3B42, PERSIANN-CDR, CFSR, ERA-5, CPC) has been previously evaluated (AL-Falahi et al., 2020) against daily and monthly observations form various locations to address data limitation. Among the investigated products, CHIRPS was identified as the most accurate gridded product at daily, monthly, and annual timescale and showed strong correlation and low biases against ground observations (AL-Falahi et al., 2020). CHIRPS is available at 0.05° from 1981 to present and can be downloaded from the Climate Hazards Group (CHG), UC Santa Barbara (https://data.chc.ucsb.edu/products/CHIRPS-2.0/).

2.1.2. Reanalysis data

Historical predictors (1991–2020) derived from the reanalysis data of the National Center for Environmental Prediction/the National Center for Atmospheric Research (NCEP-NCAR 1) were used for the calibration and validation of the Statistical Down-Scaling Model (SDSM). For this study, the NCEP-NCAR data comprised 26 atmospheric variables such as specific humidity, wind direction, and mean temperature (Table 1). These data can be accessed from the National Oceanic Atmospheric Administration (https://psl.noaa.gov/data/gridded/data.ncep.reanalysis.html) as well as from the SDSM Statistical Downscaling Model home page (https://sdsm.org.uk/data.html).

Table 1
NCEP predictors used for model calibration and validation.

No	Code	Long name	No	Code	Long name
1	mslp	Mean sea level pressure	**14**	p5zh	500 hPa divergence
2	pl_f	Surface airflow strength	**15**	p8_f	850 hPa airflow strength
3	pl_u	Surface zonal velocity	**16**	p8_u	850 hPa zonal velocity
4	pl_v	Surface meridional velocity	**17**	p8_v	850 hPa meridional velocity
5	pl_z	Surface vorticity	**18**	p8_z	850 hPa vorticity
6	plth	Surface wind direction	**19**	p850	850 hPa geopotential height
7	plzh	Surface divergence	**20**	p8th	850 hPa wind direction
8	p5_f	500 hPa airflow strength	**21**	p8zh	850 hPa divergence
9	p5_u	500 hPa zonal velocity	**22**	Prcp	Precipitation
10	p5_v	500 hPa meridional velocity	**23**	s500	Specific humidity at 500 hPa
11	p5_z	500 hPa vorticity	**24**	s850	Specific humidity at 850 hPa
12	p500	500 hPa geopotential height	**25**	Shum	Surface specific humidity
13	p5th	500 hPa wind direction	**26**	Temp	Mean temperature at 2 m

2.1.3. Global climate models (GCMs) data

For building future scenarios of precipitation potential changes, rainfall historical data and predictors (1991–2020) derived from the second-generation Canadian Earth System Model (CanESM2) and the Canadian Earth System Model Version 5 (CanESM5) were downloaded to assess their accuracy during the validation period relative to ground observations and the historical output of SDSM. This assessment was crucial in determining the most accurate model to employ for building future scenarios. In this study, we illustrate the potential change of future precipitation under two representative concentration pathways (RCPs); RCP2.6 and RCP8.5 for the period (2026–2100). The remaining RCPs such as RCP4.5 and RCP3.6, represent intermediate pathways with simulated values falling between those of RCP2.6 and RCP8.5.

The RCP2.6 is a low-emission scenario (Chaturvedi et al., 2012; Vuuren et al., 2011). The carbon dioxide emissions (CO_2) under RCP2.6, according to the IPCC fifth assessment report (AR5) (IPCC, 2013), are assumed to decline by 2020 and go to zero by 2100. It also requires that the Sulphur dioxide (SO_2) emissions decline to approximately 10 % of those of 1980–1990 and methane emissions (CH_4) will go to approximately half the CH_4 levels by 2020. Therefore, RCP2.6 is likely to keep global temperature rise below 2 °C by 2100 (Gasser et al., 2015; Sanderson et al., 2016). Under RCP8.5, emissions will continue to rise throughout the 21st century. RCP8.5 is the worst-case climate change scenario based on what is confirmed to be an overestimation of projected coal outputs. According to the RCP8.5, the global mean temperature is projected to rise by 3.8 °C by the late-21st century (Baek et al., 2013). The RCPs can be downloaded from the Canadian Climate Data and Scenarios website (http://climate-scenarios.canada.ca/)

2.1.4. Assessment of GCMs ensembles (CMIP5 and CMIP6)

To ensure the consistency of SDSM output with GCMs, the SDSM output was assessed across the historical and future periods. The ensemble means of GCMs from CMIP5 and CMIP6 for the period 1991–2020 and 2026–2100 were utilized to evaluate the SDSM output. Historical and the precipitation projected mean from 44 GCMs (Table 2) of the Coupled Model Inter-comparison Project Phase 5 (CMIP5) and their updated version from the Coupled Model Inter-comparison Project Phase 6 (CMIP6) were retrieved from the Canadian climate data and scenarios data portal at a spatial resolution of 1° and used for evaluation against ground observations and SDSM output. Under CMIP6, we

Table 2
A list of GCMs (CMIP5) and (CMIP6*) used for assessment against historical observations and future scenarios of SDSM.

Model Name	Institution	Spatial Res.	Model Name	Institution	Spatial Res.
BCC-CSM1.1	Beijing Climate Center (China)	2.8° × 2.8°	BCC-CSM1.1(m)	Beijing Climate Center (China)	1.12° × 1.12°
BCC-CSM2-MR*	China Meteorological Administration	2.8° × 2.8°			
BNU-ESM	College of Global Change and Earth System Science (China)	2.8° × 2.8°	FGOALS-g2	LASG-CESS (China)	2.8° × 2.8°
			FGOALS-g3*	LASG-CESS (China)	2° × 2.3°
CanESM2	Canadian Centre for Climate Modeling and Analysis (Canada)	2.8° × 2.8°	GFDL-CM3	NOAA Geophysical Fluid Dynamics Laboratory (USA)	2° × 2°
CanESM5*		2.8° × 2.8°			
CCSM4	National Center for Atmospheric Research (USA)	1° × 1°	GFDL-ESM2G	NOAA Geophysical Fluid Dynamics Laboratory (USA)	2° × 2.5°
			GFDL-ESM4*		1.3° × 1°
CESM1	(BGC) Community Earth System Model Contributors (USA)	1.3° × 0.9°	GFDL-ESM2M	NOAA Geophysical Fluid Dynamics Laboratory (USA)	2° × 2.5°
CESM2*		1.3° × 0.9°			
CNRM-CM5	Centre National de Recherches Météorologiques (France)	1.4° × 1.4°	HadGEM2-AO	Met Office Hadley Centre (UK)	1.25° × 1.9°
CNRM-CM6-1*		1.4° × 1.4°			
CSIRO-MK3.6.0	CSIRO-QCCCE (Australia)	1.8° × 1.8°	HadGEM2-ES	Met Office Hadley Centre (UK)	1.25° × 1.9°
IPSL-CM5A-LR	Institut Pierre-Simon Laplace (France)	1.9° × 3.75°	IPSL-CM5A-MR	Institut Pierre-Simon Laplace (France)	1.25° × 1.25°
IPSL-CM6A-LR*			IPSL-CM6A-LR*	Institut Pierre-Simon Laplace (France)	1.25° × 1.25°
MIROC-ESM	MIROC (Japan)	2.8° × 2.8°	MIROC-ESM-CHEM	MIROC (Japan)	2.8° × 2.8°
MIROC6*		1.4° × 1.4°			
MIROC5	MICRO (Japan)	1.4° × 1.4°	MPI-ESM-MR	Max-Planck-Institut für Meteorologie (Germany)	1.9° × 1.9°
			UKESM1-0-LL*	Hadley Centre (UK)	1.9° × 1.3°
MPI-ESM-LR	Max-Planck-Institut für Meteorologie (Germany)	1.9° × 1.9°	MRI-CGCM3	Meteorological Research Institute (Japan)	1.1° × 1.1°
MPI-ESM1-2-LR*		1.9° × 1.9°			
NorESM1-M	Norwegian Climate Centre (Norway)	2.5° × 1.9°	FIO-ESM	First Institute of Oceanography, State Oceanic Administration FIO (China)	1.25° × 0.9°
		2.5° × 1.9°			
NorESM2-LM*	Norwegian Climate Centre (Norway)		FIO-ESM-2-0*		1.25° × 0.9°
GISS-E2-R	NASA Goddard Institute for Space Studies (USA)	2° × 2°	GISS-E2-H	NASA Goddard Institute for Space Studies (USA)	2° × 2.5°
			GISS-E2-1-H*		
EC-EARTH2	European Centre for Medium-Range Weather Forecasts (ECMWF)	1.12° × 1.12°	CNRM-CM6-1*	Centre National de Recherches Meteorologiques Meteo-France, France	0.4° × 0.4°
EC-Earth3*	European consortium	0.7° × 0.7°			

examined Shared Socioeconomic Pathways (SSPs) the updated versions of the selected RCPs to explore the progress made on CMIP6 in comparison with CMIP5.

SSPs are the new pathways that examine how global society, demographics, and economics might change over the next century (Maury et al., 2017; O'Neill et al., 2015). We have selected SSP126 and SSP585, the updated versions of RCP2.6 and RCP8.5. SSP126 represents the low end of the range of plausible future pathways. The scenario depicts the "best case" future from the sustainability perspective (Eyring et al., 2015). The SSP585 represents the high end of plausible future pathways and is the only SSP with emissions high enough to produce the 8.5 W/m^2 level of forcing in 2100 (Fettweis et al., 2021; Riahi et al., 2016). The output of the GCMs driven by each SSP can be obtained from the ESGF website; (https://esgf-data.dkrz.de/search/cmip6-dkrz/). This assessment against GCMs helped us to identify which models are showing the possible change and to calculate the percentage of the bias based on the current climate.

2.2. The Statistical Down-Scaling Model (SDSM)

Statistical Down-Scaling Model (SDSM) is a hybrid of transfer function and weather generation model (Wilby and Dawson, 2007). The model has received more attention during the last decade due to its applicability in impact and assessment studies (Hassan et al., 2014; Wilby et al., 2014). The model has been used by many scientists and climate experts to synthesize daily weather series climate future parameters, such as precipitation and temperature, and also to investigate the possible impact of climate change on the water cycle (Saddique et al., 2019a,b; Sennikovs and Bethers, 2009).

The SDSM develops a statistical relationship between predictors (global variables) and predictands (local parameters) using a multi-linear regression method, while the systematically generated biases by GCM predictors can be reduced and normalized in the SDSM during the calibration period (Wilby and Dawson, 2007). Multiple processes can be performed by SDSM such as data quality control, model calibration, screening of predictors, bias correction, and scenario generation. SDSM can be calibrated at annual, monthly, and seasonal time scales according to the length of observed data.

In the recent study, SDSM was calibrated under the conditional model method. Under this process, SDSM builds an intermediate connection between the large-scale forcing predictors (e.g., specific humidity, wind direction) and local predictand (precipitation) (Wilby et al., 2002). Further, the ordinary least square (OLS), bias correction with value 1, and variance inflation 12 were specified to optimize model performance.

During the screening of predictors, the most important and challenging task in SDSM, (Akhter et al., 2018; Rashid et al., 2014; Gebrechorkos et al., 2019a,b), the predictors were selected based on their high agreement and correlation with the predictand (precipitation) at statistical significance ($P < 0.05$), as well as partial correlation analysis of the predictand-predictor relationship. A number of predictors such as specific humidity at 850 hpa (s850), zonal velocity (p8_u), and surface zonal velocity (p1_u), were selected to calibrate the model and to generate daily ensembles in each station using the linear regression and stochastic method of bias correction techniques (Tavakol-Davani et al., 2013). After the most correlated predictors were identified and the calibration was completed (at daily and monthly timescale), the calibrated parameters were employed in the validation step. In this study, the future projection of precipitation variability is divided into three projection periods; 2026–2050 (2030s); 2051–2075 (2060s); and 2076–2100 (2090s).

Further, the accuracy and credibility of SDSM during the calibration

and validation periods, as well as in the future projection periods were evaluated by weighting the difference between downscaled and observed precipitation using different statistical methods included in the model, and also by computing other related statistical methods such as coefficient of determination (R^2, eq., **1**), Bias (eq., **2**), Percent of Bias (Pbias, eq., **3**), and Root Mean Square Error (RMSE, eq., **4**);

$$R^2 = \frac{\sum_{i=1}^{N}(P_i - \overline{P})\cdot(O_i - \overline{O})}{\sqrt{\sum_{i=1}^{N}(P_i - \overline{P})^2}\cdot\sqrt{\sum_{i=1}^{N}(O_i - \overline{O})^2}} \quad (1)$$

$$Bias = \frac{\Sigma_{i=1}^{N}(P_i - O_i)}{N} \quad (2)$$

$$Pbias = \frac{\Sigma_{i=1}^{N}(P_i - O_i)}{\Sigma_{i=1}^{N}(O_i)} \times 100 \quad (3)$$

$$RMSE = \frac{\sqrt{\Sigma_{i=1}^{N}(O_i - P_i)^2}}{N} \quad (4)$$

Where, O_i and P_i are observed and modeled values, respectively. $\overline{O}$ and $\overline{P}$ are the average of observed and modeled values, respectively and N is the number of data points. In addition, a linear scaling bias correction was used to adjust the potential bias present in the projected precipitation values.

3. Results

3.1. Calibration and validation of the model

For calibration and validation of the accuracy of SDSM, we compared its outputs, using NCEP predictors, with observational data for the periods 1991–2010 and 2011–2020 at both monthly and daily timescales, respectively. Fig. 2 presents summary statistics from the SDSM calibration, including monthly mean, monthly sum, monthly maximum, variance, percent of wet days, 95th percentile, and mean spell length (days). These statistics provide a comprehensive assessment of SDSM performance.

The coefficient of determination (R^2) showed strong agreement between SDSM simulated estimates and the observed precipitation with a value of 0.98 (Table 3). The same result is also observed with the occurrence of wet days $R^2 = 0.98$, mean $R^2 = 0.95$, and the variance $R^2 = 0.93$. A relatively higher variation is observed between the observed data and simulated mean wet spell length $R^2 = 0.70$. The occurrence of wet days, mean, and wet spell length showed root mean square error (*RMSE)* of 0.026 mm, 0.46 mm, and 0.32 mm, respectively. In addition, the total rainfall and variance show a *RMSE* of 3.14 mm and 2.78. Given these outcomes, the SDSM slightly overestimates the rainfall total *Pbias* = 8.45 % and underestimates wet spell lengths *Pbias* = −18.8 %.

Table 3
Statistical analysis result of SDSM performance against observations during the calibration period.

Value	R^2	RMSE	Pbias (%)
Mean (mm)	0.95	0.46	0.95
Sum (mm)	0.98	3.14	8.45
Wet days (%)	0.98	0.026	−7.13
Variance	0.93	2.78	−9.54
Mean wet spell length (days)	0.70	0.32	−18.86

At a daily timescale (Table 4), the mean value of the daily observations and simulated values of SDSM is 5.05 mm and 5.40 mm with an *RMSE* of 4.5. The *Pbias* is 6.3 % and the standard deviation of observations and SDSM values is 6.78 mm, and 7.49 mm, respectively.

For the validation step, we used an independent daily dataset from 2011 to 2020 that was not included in the model's calibration process. The SDSM demonstrated substantial performance in generating daily estimates that closely matched the observed data. The model achieved a root mean square error (*RMSE*) of 7.6 mm and a percent bias (*Pbias*) of −6.2 %, indicating a small deviation from the observed values. The standard deviation of the model outputs (9.21 mm) was also comparable to the observed data (8.73 mm). Furthermore, the coefficient of determination (R^2) between the SDSM estimates and the observations was

Table 4
Result of SDSM performance compared to observations at a daily timescale during the calibration period 1991–2010.

St. estimator	Obs.	SDSM
Mean (mm)	5.05	5.40
Standard deviation (mm)	6.78	7.49
RMSE (mm)	4.52	
Bias (mm)	0.36	
Pbias (%)	6.3	

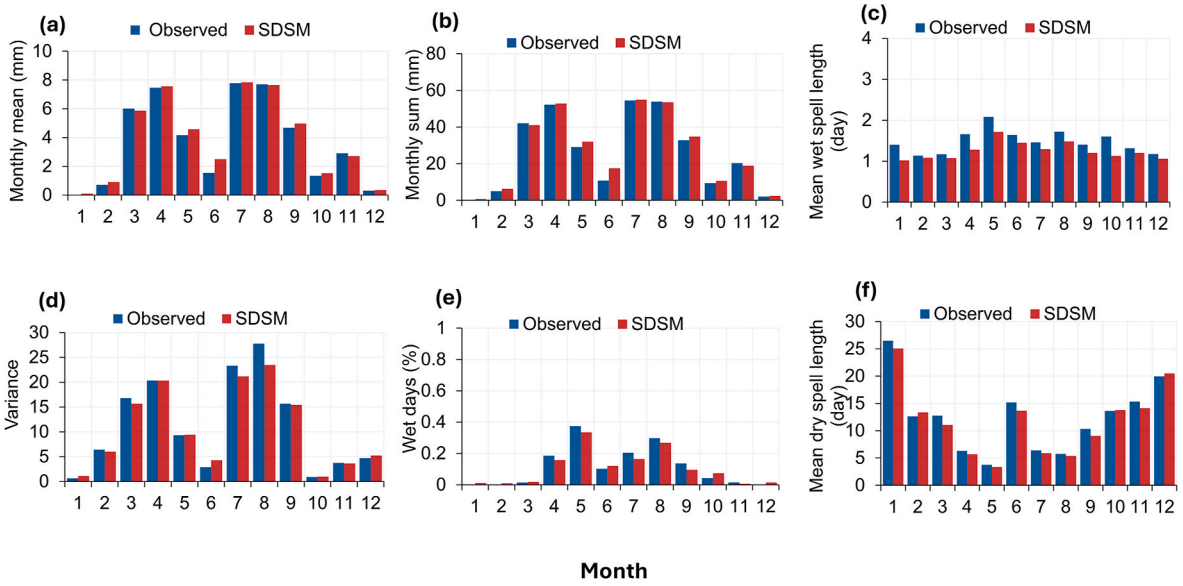

Fig. 2. Summary statistics displaying performance of SDSM compared to observed precipitation during the calibration period 1991–2010. **a**) Monthly mean **b**) Monthly sum **c**) Mean wet spell length (day) **d**) Variance **e**) Wet days (%), **f**) Mean dry spell length (day).

0.76, reflecting a good agreement between the two datasets.

To develop future scenarios and identify the most suitable model under CMIP5 and CMIP6, we evaluated the performance of the Canadian Earth System Model version 2 (CanESM2-CMIP5) and its updated version, Canadian Earth System Model 5 (CanESM5-CMIP6). The evaluation involved comparing the historical outputs of both models with observed data for the period 1991–2020. The assessment revealed that both models exhibited biases in estimating rainfall over the study area, with tendencies to both overestimate and underestimate rainfall amounts. In general, the models underestimated total monthly rainfall during the two rainy seasons, while overestimating average rainfall during the drier months (Fig. 3).

The coefficient of determination (R^2) between the model outputs and observed data was 0.85 for CanESM2 and 0.62 for CanESM5. CanESM2 demonstrated a root mean square error (*RMSE*) of 14.7 mm and a percent bias (*Pbias*) of −25.3 %, while CanESM5 showed an RMSE of 16.71 mm and a Pbias of −23.8 %. Overall, CanESM2 provided precipitation estimates that were more consistent with the observed data. Therefore, CanESM2 predictors were selected for projecting future precipitation variability in the study area.

3.2. Current condition of precipitation across the region

According to the rainfall historical data (1991–2020), the average seasonal rainfall during March–May (MAM), July–August (JJA), December–February (DJF), and September–November (SON) is less than 150 mm (Fig. 4).

The outcome of the interpolated maps, employing IDW, align with previous studies performed in Yemen, which also demonstrated higher seasonal rainfall across the western regions of the study area and lower rainfall rates in the eastern zones. During the reference period, the western areas (Al Mahwit, Raymah) and the middle districts of Sana'a governorate received the highest levels of rain throughout the year. During MAM and JJA around 311 mm and 316 mm of precipitation were registered in Al Mahwit, the west of Sana'a, and Raymah governorate compared to 195 mm and 208 mm in the eastern parts (East of Sana'a, Amran, and southeastern districts of Thamar governorate). During the dry season (DJF), Amran received higher rates of rainfall compared to the rest districts of the region. During the moderate rainfall season (SON), the western zone of the region showed the highest rates of precipitation, particularly Raymah governorate, with averages around 60.37 mm compared to 29.37 mm in the east and southeastern part of the region, namely east of Sana'a and Thamar governorate.

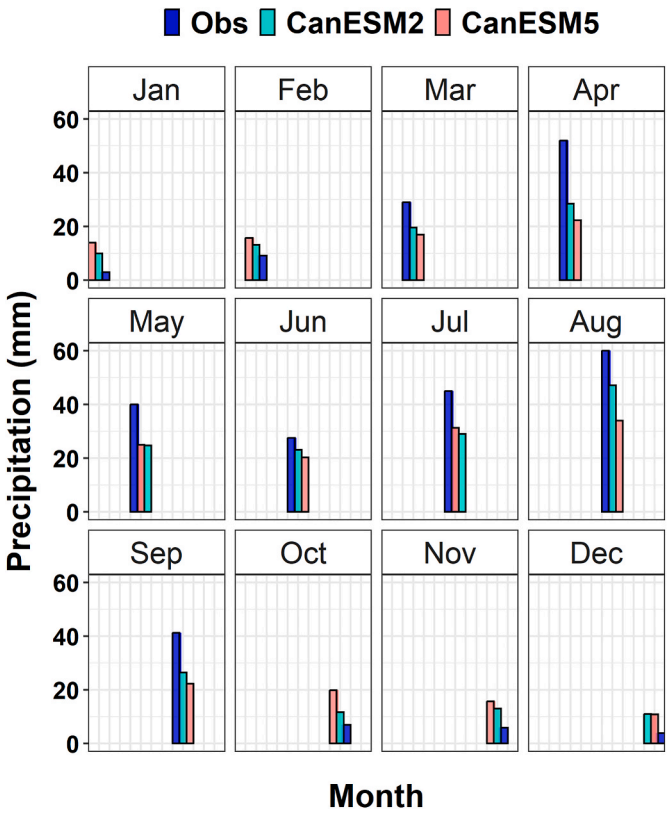

Fig. 3. Precipitation historical estimates (1991–2020) by CMIP5 model (CanESM2) and CMIP6 (CanESM5) relative to the area averages of the observed total precipitation. As shown, both models (CanESM2 & CanESM5) underestimate heavy precipitation events or overestimate light rains compared to actual observations. However, CanESM2 demonstrated a closer correlation with the observations, particularly in the rainy months.

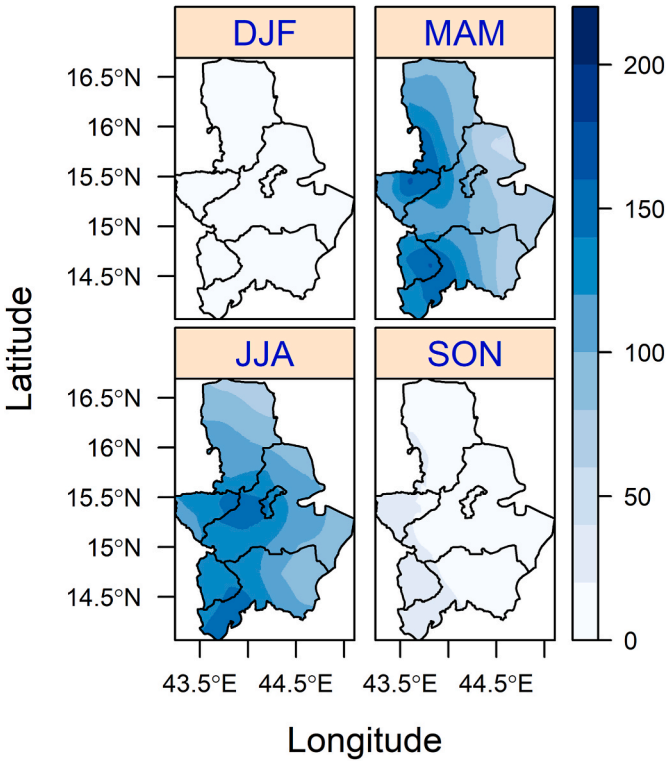

Fig. 4. Precipitation seasonal averages based on the reference period (1991–2020). Rates of rainfall during March through May (MAM), June to August (JJA), and September through November (SON) are more substantial in the western zones of the region.

3.3. Future scenarios

Precipitation projections under RCP2.6 and RCP8.5 indicate significant changes in seasonal rainfall compared to the past. While the magnitude of change varies notably between governorates, the patterns remain relatively consistent across the four seasons examined under both scenarios.

3.3.1. Seasonal projections

Compared to the baseline period (1991–2020), seasonal average precipitation will increase up to 180 mm over the entire region in the 2030s, 2060s, and 2090s under RCP2.6 (Fig. 5).

In the 2030s, precipitation during DJF will increase up to 7.9 % in Al Mahwit, Amran, and Raymah, while, a decrease is projected on Sana'a and Thamar governorate to −19.84 %. In MAM, the projection shows an average increase in rainfall of up to 5.9 % in Al Mahwit, east of Sana'a, Raymah, and Thamar, and an average decrease of −6.84 % in the west of Sana'a and Amran. During JJA, east of Sana'a, Amran, and Raymah will

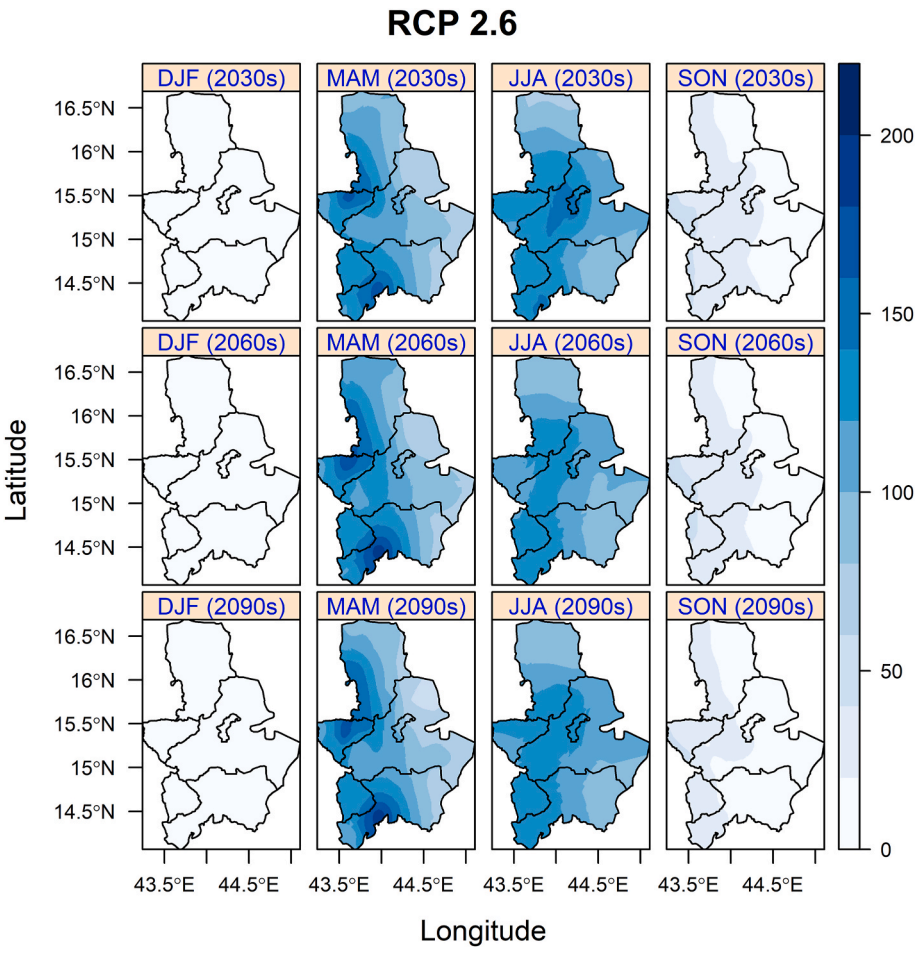

Fig. 5. Projected change in seasonal precipitation (mm) in the 2030s, 2060s, and 2090s under RCP2.6. Most of precipitation increase is projected during 2060s and 2090s across the region, with higher rates in Al Mahwit and the western districts of Thamar governorate.

experience higher precipitation up to 6.16 %. However, a slight decrease is being projected to around −2.82 % for some areas of Al Mahwit and west of Sana'a.

The greatest change in precipitation across the entire region is observed during SON, with an average percentage of 89.17 %, particularly in the east of Sana'a, Al Mahwit, and Amran governorate. This may indicate a potential increase in rainfall averages during SON over this area compared to the current time. During the 2060s, average precipitation is projected to increase in the dry season (DJF) to around 24.65 % across the region, with a potential decrease of about −12.23 % in the west of Sana'a. During MAM and JJA, precipitation is projected to increase up to 28.1 % all across the region with a minor decrease in the west of Sana'a. In SON, the result is identical to the findings during the 2030s. The percentage of change shows a significant increase up to more than 80 %. In the 2090s, the precipitation is projected to increase with a slight decrease of about −9.3 % during DJF in some districts within the western part of Sana'a governorate and −11.4 % during SON in Raymah. The overall increase during the 2090s is 22.27 %, 16.72 %, 6.7 %, and 36.89 % during DJF, MAM, JJA, and SON, respectively. The highest percentage of change in precipitation is projected during the 2060s in the eastern parts of Sana'a, Al Mahwit, and Amran.

In the case of RCP8.5, precipitation is projected to increase at higher rates than those estimated under RCP2.6.

The projection during the 2030s showed increased precipitation in MAM, JJA, and SON up to 13.91 %, 10.21 %, and 92.35 %. A considerable change is being observed during SON, particularly in Sana'a governorate and Al Mahwit (Fig. 6). A decrease in precipitation is projected during the dry season (DJF) up to −14.10 % in some parts of Sana'a governorate. During the 2060s and 2090s, the precipitation is projected to increase in all seasons with no significant decrease. Projected change during DJF, MAM, JJA, and SON in the 2060s is 40.37 % 22.04 %, 23.83 %, and 120 %, respectively. In the 2090s, the precipitation during DJF will increase up to 78 % all across the region. Raymah and Thamar governorate will experience much of this increase during DJF season. During the same period (2090s), a substantial increase is projected in MAM on Al Mahwit and Thamar up to 56.43 % and up to 55.1 %. The other governorates (Sana'a, Amran, Raymah) will experience an increase during the 2090s up to 42.18 %, 53.4 %, and 97.9 % in MAM, JJA, and SON, respectively. The pronounced increase during the 2090s is projected in September, particularly over Sana'a governorate (170 %), Amran (153 %), and Al Mahwit (112 %). However, Raymah is projected to experience a minor decrease to around −0.94 % in the 2090s during the SON season. Under RCP8.5, SDSM yielded a similar result as under RCP2.6 for the projected increase in precipitation during the SON season, but it showed the largest increase in precipitations to take place in the 2090s, while under RCP2.6 the highest precipitation over the study area is projected during the 2060s. Table 5 contains the estimates of the projected increase in precipitations during the two rainy seasons (MAM) and (JJA) compared to the reference period. The western zones of the region, namely Al Mahwit, Raymah, and the west of Sana'a are projected to experience the greatest increase in precipitation under both scenarios.

3.3.2. *Annual projections*

Through the baseline period (1991–2020), the annual mean of precipitation over the region is less than 350 mm. The lowest levels of

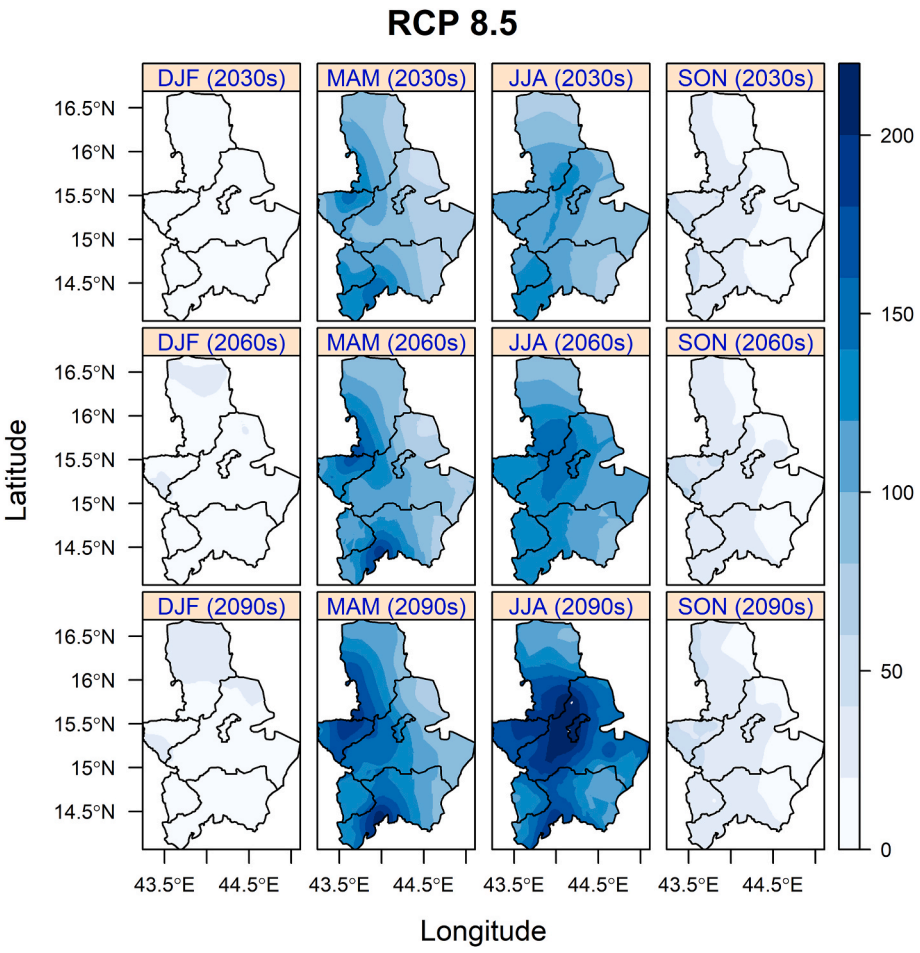

Fig. 6. Projected change in seasonal precipitation (mm) during DJF, MAM, JJA, and SON in the 2030s, 2060s, and 2090s under RCP8.5. The increase of precipitation averages is more distinct in June through August (JJA) in the 2090s over the entire region.

Table 5
Mean of the projected change in seasonal precipitation (mm) during the two rainy seasons (MAM and JJA).

Region	1991–2020 (Ref.period)		2026–2050 (2030s)				2051–2075 (2060s)				2076-2100 (2090s)			
	Obs.		RCP2.6		RCP8.5		RCP2.6		RCP8.5		RCP2.6		RCP8.5	
	MAM	JJA	MAM	JJA	MAM	JJA	MAM	JJA	MAM	JJA	MAM	JJA	MAM	JJA
Al Mahwit	101.5	101	113.6	98	116.9	107	127.1	101	123.8	121	123.5	102	159	161.2
Sana'a (W)	96.3	110	85.94	108	105.2	124	109	110	108.9	134	102.8	117	136.8	180.3
Sana'a (E)	61.6	86.6	62.33	91	67.00	94	72.9	89	72.5	104	66.0	94	88.9	150.1
Amran	89.9	77.4	87.70	82	96.5	88	102.9	87	101.8	103	99.57	85	122	125.2
Raymah	113.5	105	119.5	113	122.7	110	125.1	114	131.3	117	127.6	109	135.9	128
Thamar	82.2	91.8	85.41	85	98.22	96	107.2	95	104.5	104	101.5	94	127.2	129.3

precipitation were measured in the north and the north-eastern districts, namely Sana'a and Amran governorate with rates less than 250 mm/year, while the greatest levels of rain were observed in Al Mahwit, west of Sana'a, and Raymah governorate with averages between 300 and 350 mm/year.

Future projections showed a substantial increase in precipitations in the annual scale by both scenarios. The increased precipitation is more distinct in the western districts and extends at a relatively good amount towards the east, especially under RCP8.5 in the 2060s and the 2090s. Under RCP2.6, the annual averages in the 2030s will increase up to 201.3 mm in Amran, 174.74 mm in the eastern districts of Sana'a, 221 mm in the west of Sana'a, and 150 mm in Thamar governorate. In Al Mahwit and Raymah governorate, the projected increase is around 270.13 mm and 260 mm, respectively. During the 2060s, Raymah and Al Mahwit exhibited the highest levels of precipitation up to 275 mm/year.

The projected increase in the west of Sana'a is 250 mm, Amran 222.56 mm, and around 185.6 mm in the eastern districts of Sana'a. During the 2090s, Raymah showed higher precipitation averages compared to the other governorates with precipitation rates around 270.6 mm/year. Al Mahwit, west of Sana'a, Thamar, Amran, and east of Sana'a are projected to receive annual averages of about 265.7 mm, 245.48 mm, 217.31 mm, 213.39 mm, and 178.9 mm. However, the precipitation averages in Al Mahwit during the 2090s are less than the rates projected in the 2060s.

In the case of RCP8.5, a further increase in precipitation is predicted during the 2030s, 2060s, and 2090s. In the 2030s, precipitation will increase up to 273 mm/year in Al Mahwit and Raymah governorate. While in the west of Sana'a, Thamar, and Amran, as well as in the eastern districts of Sana'a, the increased estimates are around 261 mm, 221.9 mm, 215.6 mm, and 182.69 mm/year, respectively. During the

2060s, most of Al Mahwit districts and west of Sana'a will receive substantial rates of precipitation with averages around 305 mm and 280 mm. The future projected changes in Raymah, Amran, Thamar, and east of Sana'a are 284.6 mm, 244 mm, 241.5 mm, and 204.4 mm. The greatest increase in precipitation is expected to occur during the 2090s. All districts of the region will receive higher rainfall rates between the period 2076 and 2100. For example, Al Mahwit and the west of Sana'a will experience a substantial increase in precipitation up to 378 mm. Large parts of Thamar governorates, especially the western districts, are projected to receive between 290 and 320 mm/year. In Raymah, Amran, and the east of Sana'a, increased precipitation up to 289 mm is projected. Overall, the annual increase in the average precipitation levels under RCP8.5 is 450 mm compared to 300 mm in the reference period.

3.3.3. Comparison with GCMs

To further evaluate the accuracy of SDSM, the averages from the reference period (1991–2020) were analyzed alongside the ensemble means of GCMs and compared against observed precipitation data. For future projection, scenarios of CMIP5 and CMIP6 ensemble means were assessed in comparison with the future output of SDSM for the period (2026–2100).

The result shows that GCMs from both CMIP5 and CMIP6 tend to over and underestimate precipitations compared to SDSM (Fig. 7). The historical output generated by SDSM against the observations exhibits a percent bias of less than −4 % compared to −15.34 % and −27.6 % by CMIP5 and CMIP6, respectively. In future projections, the originated bias by CMIP5 and CMIP6 models further decreased, bringing their output closer to SDSM projections. In the 2030s, the average deviation under RCP2.6 and RCP8.5 for CMIP5 is −11.75 %, while under SSP126 and SSP585, CMIP6 shows an average bias of −13.86 %.

In the 2060s and 2090s, CMIP6 projections demonstrated greater relevance compared to CMIP5. The average Pbias values, as indicated in Table 6, are 2.49 and −9.47 under SSP126 and SSP585 during the 2060s and 2090s, respectively. During the same period, the average value of Pbias for CMIP5 is −18.45 and −12.38 under both RCPs. CMIP6 showed greater consistency with SDSM output in producing future precipitation estimates across the region compared to CMIP5. In CMIP6 additional forced factors have been included such as emissions of anthropogenic activities along with emissions of short-lived species and long-lived greenhouse gases (Eyring et al., 2015; Gidden et al., 2019). This side

Table 6
Result of Pbias (%) showing deviation between mean of GCMs & SDSM projections.

Data	SDSM	GCMs (CMIP5)	GCMs (CMIP6)
Historical	(−3.96)	(−15.34)	(−27.61)
2030s		RCP2.6 (−13.2)	SSP126 (−14.6)
		RCP8.5 (−10.30)	SSP585 (−13.13)
2060s		RCP2.6 (−17.1)	SSP126 (−8.12)
		RCP8.5 (−19.8)	SSP585 (13.1)
2090s		RCP2.6 (−17.42)	SSP126 (−13.60)
		RCP8.5 (−7.34)	SSP585 (−5.34)

was not fully integrated into CMIP5. Also, abruptly quadrupling CO_2 simulation is included for the first time in CMIP6, which suggests that 1 % of CO_2 increased throughout the entire simulation (1 % a year) rather than keeping it constant as in CMIP5 (Eyring et al., 2015; Winton et al., 2020).

4. Discussion

The impact of climate change at the global level is evident, primarily the rise of temperature (Baliram and Jadhav, 2020; Gambo Hamza et al., 2020), but uncertain at the local level especially the precipitation variability (Giorgi, 2010; Refsgaard et al., 2013). It is still not clear whether the change in the climate will affect local variables such as precipitation (Ashmore and Church, 2001; Li et al., 2013). The absence of accurate studies at a local level along with the uncertainties of GCM projections (Lehner et al., 2019; Thompson et al., 2013), makes future projections at the regional and local level, imprecise (Racherla et al., 2012). Even though the application of a single GCM is a common practice in some impact assessment studies (Abbasnia and Toros, 2016; Hashmi et al., 2010; Souvignet et al., 2010), projections produced by most GCMs are not recommended for local impact studies because of their coarse resolution (>100 km) and the difficulty to integrate local forcing factors, such as complex topography and wind movement (Onol, 2012; Saddique et al., 2019a,b; Tsegaw et al., 2020). Due to these limitations, more practical and accurate methods have been developed such as the downscaling techniques, mainly the statistical down-scaling (SDSM), which has been widely used in several studies (Gagnon et al., 2005; Hussain et al., 2015; Tahir et al., 2018) for its high performance in

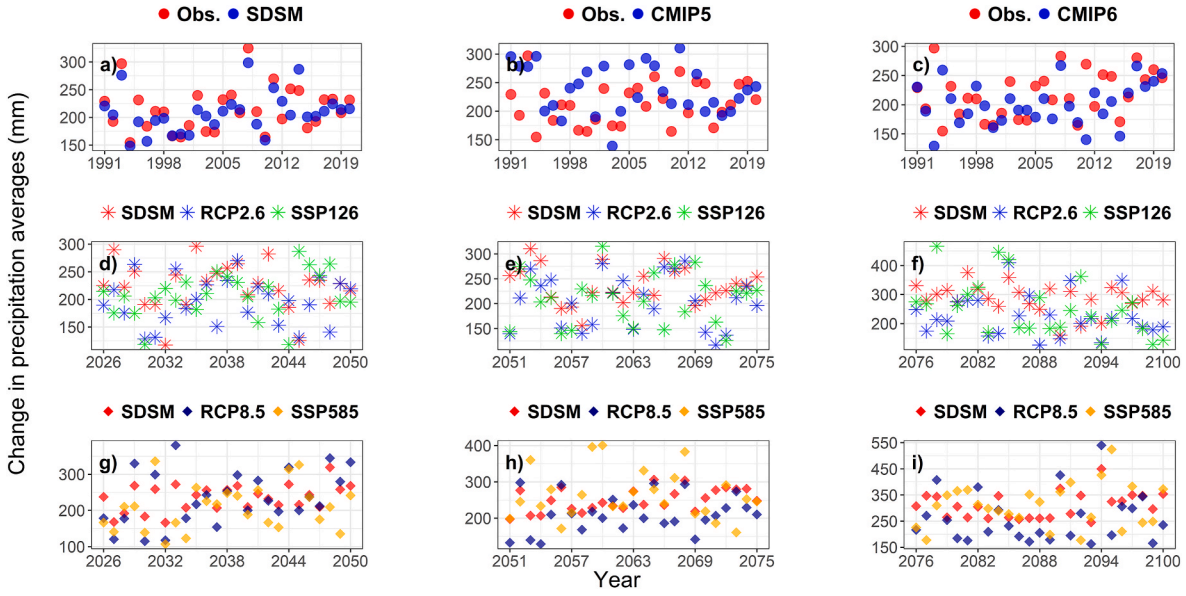

Fig. 7. Assessment of average annual precipitation (mm) by a) SDSM, b) ensemble mean of CMIP5, c) ensemble mean of CMIP6 against the historical observations for the reference period (1991–2020). Figures d to i illustrate the comparison analysis of CMIP5 and CMIP6 compared to SDSM output for the 2030s, 2060s, and the 2090s.

reproducing estimates equivalent to past values and generation of reasonable projections in the future.

This study demonstrated that downscaling using SDSM provides a more detailed and reliable understanding of future precipitation changes in the highland region of Yemen. The results suggest a significant increase in precipitation over the next century, particularly in the western provinces (Al Mahwit, Raymah, west of Thamar, and west of Sana'a). This is likely due to local and regional climatic influences, such as the Inter-Tropical Convergence Zone (ITCZ) and the Red Sea Convergence Zone (RSCZ), as well as expected increases in greenhouse gas emissions that would affect the local climate towards more precipitations across the region, in particular during the 2060s and the 2090s. So, it is likely that climate change will increase the frequency and severity of extreme weather events such as droughts, flash floods, and sandstorms (Al-Jawaldeh et al., 2022). This conclusion is consistent with studies presented by (Hasanean and Almazroui, 2015), which suggest a potential increase in the annual averages of rainfall in the southwestern areas of the Arabian Peninsula. The same study points out that the future increase in precipitation across the region is influenced by El Niño Southern Oscillation (ENSO) and other circulations such as centers of high and low pressure and the North Atlantic Oscillation (NAO).

In the meantime, the percentage of change in precipitation is more pronounced during September compared to other months, which implies a possible shift in precipitation timing. A shift in precipitation timing is, however, reported in similar studies conducted in some other semi-arid regions (Huang et al., 2011; Mahmood and Mukand, 2012; Saddique et al., 2019a,b). In addition, the projected precipitation by SDSM is in line with precipitation trends of some GCMs, which were previously utilized in Yemen (Al-Jibly, 2008; Bosworth et al., 2005; EPA, 2013) and along with studies covering the Arabian peninsula, although notable differences in magnitude exist between SDSM and those of other models. In general, most of the employed GCMs in Yemen agreed on the potential occurrence of frequent and intense rainfall events, therefore posing an increased risk of floods (EPA, 2013).

This study observed a similar trend in the projections of GCMs under CMIP5 and CMIP6. Both projects over/underestimated historical precipitations and demonstrated large variations in future simulations in comparison with SDSM output (Fig. 7). Further, CMIP6 produced more accurate precipitation estimates in the future identical to SDSM output, which may imply the progress being made on the CMIP6 project phase compared to CMIP5. Compared to SDSM, the larger variability produced by GCMs can be attributed to the complex topography of the study area and the fact that GCMs provide area-averaged data rather than point-specific information (Gebrechorkos et al., 2019a,b; Wang et al., 2021; Yazdandoost et al., 2020). The lower performance of CanESM5 may also be due to its sensitivity. According to (Swart et al., 2019), the Equilibrium Climate Sensitivity (ECS) has changed widely within all CMIP6-GCMs. CanESM5, in particular, has a higher climate sensitivity and responds more rapidly to external forcing than CanESM2, which may have influenced its results in this study. This higher sensitivity, coupled with the inherent complexities of the region's topography, likely contributed to the model's discrepancies.

In Yemen and according to (Wilby et al., 2009), the future of precipitation across the highlands of Yemen will be affected by two factors that are expected to produce greater rainfall; the trade winds that blow in moist air from the Indian Ocean; and the steep increase in elevation. The northwest trade winds blow during April and May (entering the Red Sea Convergence Zone (RSCZ), producing the *Kharif* rains. Later in the summer, the sun moving north warms the climate and creates a trough of low pressure-the Inter-Tropical Convergence Zone (ITCZ).

Despite the promising increase in precipitation future averages over most parts of the region, the steady rise of the global temperature is expected to cause an increase in evaporation rates of soil moisture, increased prolonged hot nights, and may result in a considerable effect on the ecological systems in the region. The increased evapotranspiration may cause water stress and result in a reduction in crop yield. Moreover, certain pests and diseases are expected to thrive as a result of the warmer nights. Therefore, Yemeni farmers will need to protect the growing crops through the application of various pesticides and herbicides. Under the limited resources available to farmers for adopting advanced technology and modern methods, indigenous farming and traditional measures, which have been an integral part of the Yemeni farming heritage, could be the most effective means for minimizing the future impact of climate change.

Given the projected precipitation increases and variability, effective water resource management will be crucial for ensuring sustainable agricultural production and mitigating flood risks. Future strategies should focus on enhancing water harvesting techniques, optimizing irrigation systems, and improving watershed management. Traditional water conservation methods, such as spate irrigation and terracing, have long been utilized in Yemen and should be integrated with modern hydrological modeling to improve water storage efficiency. Additionally, investment in small-scale water reservoirs and the rehabilitation of existing ones will be necessary to maximize water retention during wet periods and ensure availability during dry spells.

Moreover, urban and rural planning should incorporate climate-resilient water infrastructure to manage extreme precipitation events effectively. The increased likelihood of intense rainfall events necessitates the enhancement of flood control measures, such as reinforced drainage systems and early warning mechanisms for flash floods. Strengthening institutional frameworks and governance for water resource management will also be essential in ensuring coordinated and sustainable responses to climate-induced water challenges.

The methods and findings of this study have broader applicability beyond Yemen, particularly for semi-arid and topographically complex regions facing similar challenges. Integrating high-resolution gridded datasets like CHIRPS with downscaling techniques provides a robust framework for localized climate projections. This method helps connect global climate models with regional adaptation needs, particularly in areas with limited data and challenging topography that obstruct precise climate evaluations. For instance, countries in the Horn of Africa, the Middle East, and parts of South Asia could benefit from adopting this methodology to improve water resource planning and disaster management strategies.

5. Summary and conclusion

For many developing countries, the down-scaling technique is the most applicable method to predict the potential impact of climate change at the local level, especially with the presence of many challenges and local obstacles such as the low numbers of meteorology stations, length of the historical observations, and poor documentation of collected data by the local agencies. The SDSM is among the best-applied approaches to study the potential impact of climate change at the local level (e.g., watershed) based on its simple applicability and low resource requirements, except the essential need for field daily-long-data (>30 years), and the indispensable time needed to select the best-correlated predictors during model calibration, in every single station.

In this study, the performance of SDSM during the calibration and the validation under both, NCEP and CanESM2 predictors at a daily time scale and incorporation of monthly means of GCMs was competent with a coefficient of determination (R^2) average of about 88 %. The projected changes in precipitation by SDSM, CMIP5, and CMIP6 models exhibit increased precipitation in the region in the 2030s with further increases in the 2060s and the 2090s. This outcome is in line with the conclusion of studies conducted earlier over Saudi Arabia and the Arabian Peninsula, where potential increases in precipitation over the south-western region of the Arabian Peninsula are projected by several global models (Almazroui et al., 2020), even with the large variations by models under CMIP6. Compared to SDSM, CMIP5 and CMIP6 global models over and underestimated precipitation amounts during the three projected

periods and displayed high deviation from the long-term historical averages of the ground observations.

According to SDSM, the annual precipitation averages will be higher than the baseline period during the three projected periods; 2030s, 2060s, and the 2090s up to 450 mm/year. The western zones of the region are projected to experience the highest precipitation levels during the 2060s and the 2090s up to 16 % and 14 % during MAM under RCP2.6, and up to 17 % and 39.44 % under RCP8.5. In JJA the projected increase is 3.83 % and 7.13 % during the 2060s and the 2090s under RCP2.6, and up to 18.22 % and 48.13 % under RCP8.5.

This concludes that the highland region of Yemen will experience more precipitations in the future, which would result in more water available for agriculture, but also risks such as floods and soil erosion are potential. The western parts of the region are projected to experience the highest precipitation rates during the 2060s and the 2090s up to 16 % and 14 % during MAM under RCP2.6, and up to 17 % and 39.44 % under RCP8.5. In JJA the projected increase is 3.83 %, and 7.13 % during the 2060s and the 2090s under RCP2.6, up to 18.22 %, and 48.13 % under RCP8.5.

The findings presented in this study are expected to contribute to the improvement of water resources management plans and adaptation strategies in the region. Also, the SDSM is applied for the first time in Yemen. Therefore, the present study introduces researchers and local agencies working on water, environment, and climate change projects with an effective method to build climate change scenarios at the local level. The high spatial resolution output of SDSM can be used directly by impact assessment studies in sectors such as agriculture and water resources. This is particularly valuable in the highlands region where rainwater is crucial for rainfed agricultural development. Nevertheless, even a better natural water supply and a well-managed, site-specific cropping system cannot solve Yemen's general mismatch of irrigation needs and water availability. It might provide extra time for improving the overall governance and for a move towards slower population growth.

This study contributes to the growing body of knowledge on climate change impacts by providing fine-scale, station-level precipitation projections for Yemen's highlands. By addressing the limitations of GCMs and leveraging SDSM, the study offers insights that are critical for regional adaptation and mitigation strategies. The findings emphasize the importance of combining global and local datasets to refine climate projections and enhance their utility for decision-making at smaller scales, such as watersheds or districts. The methodology also serves as a replicable model for improving projections in data-scarce regions worldwide.

CRediT authorship contribution statement

Ali H. AL-Falahi: Writing – original draft, Validation, Software, Resources, Methodology, Investigation, Funding acquisition, Formal analysis, Data curation, Conceptualization. **Solomon H. Gebrechorkos:** Writing – review & editing, Supervision, Methodology, Conceptualization. **Naeem Saddique:** Writing – review & editing, Visualization, Supervision, Formal analysis. **Uwe Spank:** Writing – review & editing, Supervision, Project administration, Investigation. **Christian Bernhofer:** Writing – review & editing, Supervision, Methodology, Investigation, Formal analysis, Conceptualization.

Ethical approval

We declare that this manuscript is original, has not been published before, and is not currently being considered for publication elsewhere. Further, the study has not been split up into several parts, and there is no violation of the rights of humans or institutions due to the use, distribution, or publication of this work. Moreover, no conflicts of interest are associated with this manuscript.

Data availability statement

This study utilized publicly available datasets from multiple sources. The CHIRPS daily rainfall products were obtained from the Climate Hazards Group InfraRed Precipitation with Station (CHIRPS) dataset, accessible at https://www.chc.ucsb.edu/data/chirps. Historical reanalysis data were sourced from the National Center for Environmental Prediction/National Center for Atmospheric Research (NCEP-NCAR 1) reanalysis dataset, available through the National Oceanic and Atmospheric Administration (NOAA) at https://psl.noaa.gov/data/gridded/data.ncep.reanalysis.html. The Representative Concentration Pathways (RCPs) data were retrieved from the Canadian Climate Data and Scenarios portal (http://climate-scenarios.canada.ca/). The study also incorporated Global Climate Model (GCM) outputs based on various Shared Socioeconomic Pathways (SSPs), which are accessible via the Earth System Grid Federation (ESGF) platform at https://esgf-data.dkrz.de/search/cmip6-dkrz/. For any additional information or inquiries, readers may contact the corresponding author.

Funding

This research did not receive any specific grant from funding agencies in the public, commercial, or not-for-profit sectors.

Declaration of competing interest

The authors declare that they have no known competing financial interests or personal relationships that could have appeared to influence the work reported in this paper.

Acknowledgment

We would like to thank the International Research Institute for Climate and Society, Columbia University (https://iridl.ldeo.columbia.edu) for making the high advanced gridded data (CHIRPS) free and accessible. Our appreciation also goes to Prof. Wilby (Department of Geography, Loughborough University, UK) for granting full access to the statistical model (https://sdsm.org.uk/data.html). We also thank the National Oceanic and Atmospheric Administration (NOAA), the Earth System Grid Federation (ESGF), the National Center for Environmental Prediction (NCEP), and the Canadian Climate Data and Scenarios (CCDS) for the historical provided data, predictors, and the scenarios used in this research. Special thank must be dedicated to the German Academic Exchange Service (DAAD) and the Technische Universität Dresden for offering the scholarship and for the direct supervision of the research orientation and analysis of the results.

Data availability

Data will be made available on request.

References

Abbasnia, Mohsen, Toros, Hüseyin, 2016. Future changes in maximum temperature using the statistical DownScaling model (SDSM) at selected stations of Iran. Model. Earth Syst. Environ.(MESE) (MESE) 2, 1–7. https://doi.org/10.1007/s40808-016-0112-z.

Akhter, Javed, Das, Lalu, Meher, Jitendra, Deb, Argha, 2018. Evaluation of different large-scale predictor-based statistical downscaling models in simulating zone-wise monsoon precipitation over India. Int. J. Climatol. 39. https://doi.org/10.1002/joc.5822.

AL-Falahi, Ali H., Saddique, Naeem, Spank, Uwe, Gebrechorkos, Solomon H., Bernhofer, Christian, 2020. Evaluation the performance of several gridded precipitation products over the highland region of Yemen for water resources management. Remote Sens. 12 (18). https://doi.org/10.3390/rs12182984.

Al-Hawshabi, Othman, El-Naggar, Salah, 2015. Vegetation patterns and floristic composition of Yemen. Life Sci. 1, 103–111.

Al-Jawaldeh, Ayoub, Nabhani, Maya, Taktouk, Mandy, Nasreddine, Lara, 2022. Climate change and nutrition: implications for the eastern mediterranean region. Int. J. Environ. Res. Publ. Health 19 (24). https://doi.org/10.3390/ijerph192417086.

Al-Jibly, Abdulmalek A., 2008. The Climate Change Scenarios for Yemen for 2050. Department of Geography, Sana'a Universty YEMEN. *Governmental report for Environmental protection Authority funded by UNDP*. 1437.
Al-Riffai, Perrihan, Breisinger, Clemens, Ecker, Olivier, Funes, Jose, Nelson, Gerald, Robertson, Richard, Thiele, Rainer, Verner, Dorte, Wiebelt, Manfred, Zhu, Tingju, 2013. Economic Impacts of Climate Change, pp. 32–78.
Alderwish, Ahmed, Al-Eryani, M., 1999. An approach for assessing the vulnerability of the water resources of Yemen to climate change. Climate Research - CClimate Res. LIMATE RES 12, 85–89. https://doi.org/10.3354/cr012085.
Almas, Ahmed A.M., Scholz, Miklas, 2006. Agriculture and water resources crisis in Yemen: need for sustainable agriculture. J. Sustain. Agric. 28 (3), 55–75. https://doi.org/10.1300/J064v28n03_06.
Almazroui, Mansour, Islam, Md, Saeed, Sajjad, Saeed, Fahad, Ismail, Muhammad, 2020. Future changes in climate over the arabian peninsula based on CMIP6 multimodel simulations. Earth Syst. Environ. 4. https://doi.org/10.1007/s41748-020-00183-5.
Ashmore, P., Church, M., 2001. The impact of climate change on rivers and river processes in Canada. Bull. Geol. Surv. Can. 1–48. https://doi.org/10.4095/211891.
Baek, Hee-Jeong, Lee, Johan, Lee, Hyo-Shin, Hyun, Yu-Kyung, Cho, Seorim, Kwon, Won-Tae, Marzin, Charline, Gan, Sun-Yeong, Kim, Min-Ji, Choi, Da-Hee, Lee, Jonghwa, Lee, Jaeho, Boo, Kyung-On, Kang, Hyun-Suk, Byun, Young-Hwa, 2013. Climate change in the 21st century simulated by HadGEM2-AO under representative concentration pathways. Asia Pac. J. Atmos. Sci. 49. https://doi.org/10.1007/s13143-013-0053-7.
Baliram, Lahane, Jadhav, Ganesh, 2020. *Climate Change*. Pune University, Pune. Department of Commerce & Life Sciences.
Bosworth, William, Huchon, Philippe, McClay, Ken, 2005. The Red Sea and gulf of aden basins. J. Afr. Earth Sci. 43, 334–378. https://doi.org/10.1016/j.jafrearsci.2005.07.020.
Breisinger, Clemens, Ecker, Olivier, Al-Riffai, Perrihan, Robertson, Richard, Thiele, Rainer, 2011. Climate Change, Agricultural Production and Food Security: Evidence from Yemen, vol. 1747.
Buhairi, Mahyoub, 2010. Analysis of monthly, seasonal and annual air temperature variability and trends in taiz city - Republic of Yemen. J. Environ. Protect. 1. https://doi.org/10.4236/jep.2010.14046.
Chaturvedi, Rajiv, Joshi, Jaideep, Jayaraman, Mathangi, Govindasamy, Balasubramanian, Ravindranath, N.H., 2012. Multi-model climate change projections for India under representative concentration pathways. Curr. Sci. 103, 791–802.
Chenet, Hugues, Ryan-Collins, Josh, Lerven, Frank van, 2021. Finance, climate-change and radical uncertainty: towards a precautionary approach to financial policy. Ecol. Econ. 183, 106957. https://doi.org/10.1016/j.ecolecon.2021.106957.
EPA, 2013. Yemen's Second National Communication under the United Nations Framework Convention on Climate Change. EPA, Republic of Yemen. *Governmental report by the Environmental protection Authority in Yemen with full fund by the Global Environmental Facility (GEF)*. 02. Sana'a.
Eyring, Veronika, Bony, Sandrine, Meehl, Gerald, Senior, C., Stevens, B., Ronald, Stouffer, Taylor, K., 2015. Overview of the coupled model Intercomparison project phase 6 (CMIP6) experimental design and organisation. Geosci. Model Dev. Discuss. (GMDD) 8, 10539–10583. https://doi.org/10.5194/gmdd-8-10539-2015.
Fan, Xuewei, Jiang, Lin, Gou, Jiaojiao, 2021. Statistical downscaling and projection of future temperatures across the loess plateau, China. Weather Clim. Extrem. 32, 100328. https://doi.org/10.1016/j.wace.2021.100328.
Fettweis, Xavier, Hofer, Stefan, Séférian, Roland, Amory, Charles, Delhasse, Alison, Doutreloup, Sébastien, Kittel, Christoph, Lang, Charlotte, Bever, Joris, Veillon, Florent, Irvine, Peter, 2021. Brief communication: reduction in the future Greenland ice sheet surface melt with the help of solar geoengineering. Cryosphere 15, 3013–3019. https://doi.org/10.5194/tc-15-3013-2021.
Fischer, Elske, Rösch, Manfred, Paul, Yule, 2010. The Highland Environment of Ḥimyarite Ẓafār (Yemen): Neo-Geographic Determinism?.
Gagnon, Sébastien, Singh, Bhawan, Rousselle, Jean, Roy, Luc, 2005. An application of the statistical DownScaling model (SDSM) to simulate climatic data for streamflow modelling in québec. Can. Water Resour. J. 30, 297–314. https://doi.org/10.4296/cwrj3004297.
Gambo Hamza, Yakubu, Ameta, Satish, Tukur, Adamu, Usman, Abdulwasiu, 2020. Overview on evidence and reality of climate change. IOSR J. Environ. Sci. Toxicol. Food Technol. 14, 17–26. https://doi.org/10.9790/2402-1407021726.
Gasser, T., Guivarch, Céline, Tachiiri, K., Jones, C., Ciais, P., 2015. Negative emissions physically needed to keep global warming below 2 °C. Nat. Commun. 6. https://doi.org/10.1038/ncomms8958.
Gebrechorkos, Solomon, Hülsmann, Stephan, Bernhofer, Christian, 2019a. Regional climate projections for impact assessment studies in east Africa. Environ. Res. Lett. 14. https://doi.org/10.1088/1748-9326/ab055a.
Gebrechorkos, Solomon, Hülsmann, Stephan, Bernhofer, Christian, 2019b. Statistically Downscaled Climate Dataset for East Africa, vol. 6. Scientific Data. https://doi.org/10.1038/s41597-019-0038-1.
GFDDR, 2011. Climate risk and adaptation country profile; vulnerability, risk reduction, and adaptation to climate change. Washington, DC 20433: the Global Facility for Disaster Reduction and Recovery in Colleboration with the Climate Change Team of the Environment. Department of the World Bank.
Gidden, Matthew, Riahi, Keywan, Smith, Steven, Fujimori, Shinichiro, Luderer, Gunnar, Kriegler, Elmar, Vuuren, Detlef, Berg, Maarten Van den, Feng, Leyang, Klein, David, Calvin, Katherine, Doelman, Jonathan, Frank, Stefan, Fricko, Oliver, Harmsen, J.H. M., Hasegawa, Tomoko, Havlík, Petr, Hilaire, Jérôme, Hoesly, Rachel, Takahashi, Kiyoshi, 2019. Global emissions pathways under different socioeconomic scenarios for use in CMIP6: a dataset of harmonized emissions trajectories through the end of the century. Geosci. Model Dev. (GMD) 12, 1443–1475. https://doi.org/10.5194/gmd-12-1443-2019.
Giorgi, F., 2010. Uncertainties in climate change projections, from the global to the regional scale. EPJ Web Conf. 9. https://doi.org/10.1051/epjconf/201009009.
Giorgi, Filippo, 2019. Thirty years of regional climate modeling: where are we and where are we going next? J. Geophys. Res. Atmos. 124 (11), 5696–5723. https://doi.org/10.1029/2018JD030094.
Gnitou, Gnim T., Tan, Guirong, Hongming, Yan, Nooni, Isaac K., Kenny, T. Lim Kam Sian, 2022. Resolution-sensitive added value analysis of CORDEX-CORE RegCM4-7 past seasonal precipitation simulations over Africa using satellite-based observational products. Remote Sens. 14 (9). https://doi.org/10.3390/rs14092102.
Gutowski, W.J., Ullrich, P.A., Hall, A., Leung, L.R., O'Brien, T.A., Patricola, C.M., Arritt, R.W., Bukovsky, M.S., Calvin, K.V., Feng, Z., Jones, A.D., Kooperman, G.J., Monier, E., Pritchard, M.S., Pryor, S.C., Qian, Y., Rhoades, A.M., Roberts, A.F., Sakaguchi, K., Urban, N., Zarzycki, C., 2020. The ongoing need for high-resolution regional climate models: process understanding and stakeholder information. Bull. Am. Meteorol. Soc. 101 (5), E664–E683. https://doi.org/10.1175/BAMS-D-19-0113.1.
Hadden, R.L., 2012. The Geology of Yemen: An Annotated Bibliography of Yemen's Geology, Geography and Earth Science. Bibliography. Army Geospatial Center, CEAGC-WSG-GIL. US Army Corps of Engineers 7701 Telegraph Road Alexandria, Virginia 22315.
Haidera, M., Noaman, Abdullah, 2010. Impact of Climate Change on Water Resources in Yemen: (Case Study: Surdud Drainage Basin).
Hamlet, Alan F., Salathe, Eric, Carrasco, P., 2010. Statistical Downscaling Techniques for Global Climate Model Simulations of Temperature and Precipitation with Application to Water Resources Planning Studies.
Hasanean, Hosny, Almazroui, Mansour, 2015. Rainfall: features and variations over Saudi Arabia, A review. Climate 3 (3), 578–626. https://doi.org/10.3390/cli3030578.
Hashmi, Muhammad, Shamseldin, Asaad, Melville, Bruce, 2010. Comparison of SDSM and LARS-WG for simulation and downscaling of extreme precipitation events in a watershed. Stoch. Environ. Res. Risk Assess. 1–10.
Hassan, Zulkarnain, Shamsudin, Supiah, Harun, Sobri, 2014. Application of SDSM and LARS-WG for simulating and downscaling of rainfall and temperature. Theor. Appl. Climatol. 116, 243–257. https://doi.org/10.1007/s00704-013-0951-8.
Huang, Jin, Zhang, Jinchi, Zhang, Zengxin, Xu, Chong-Yu, Wang, Baoliang, Yao, Jian, 2011. Estimation of future precipitation change in the yangtze river basin by using statistical downscaling method. Stoch. Environ. Res. Risk Assess. 25, 781–792. https://doi.org/10.1007/s00477-010-0441-9.
Hussain, Mubasher, Wan Yusof, Khamaruzaman, Mustafa, Muhammad, Afshar, Nasser Rostam, 2015. Application of statistical downscaling model (SDSM) for long term prediction of rainfall in sarawak, Malaysia. WIT Trans. Ecol. Environ. 196, 269–278. https://doi.org/10.2495/WRM150231.
IPCC, 2013. The physical science basis. Contribution of working Group I to the fifth assessment report of the intergovernmental panel on climate change. Intergovernmental Panel on Climate Change, Working Group I Contribution to the IPCC Fifth Assessment Report (AR5). Cambridge Univ press, New York, p. 1535.
IPCC, 2014. Synthesis Report. Contribution of Working Groups I, II and III to the Fifth Assessment Report of the Intergovernmental Panel on Climate Change. Synthesis Report. Intergovernmental Panel on Climate Change, Geneva, Switzerland, 2015.
Joetzjer, Emilie, Douville, H., Delire, Christine, Ciais, P., 2013. Present-day and future amazonian precipitation in global climate models: CMIP5 versus CMIP3. Clim. Dyn. 41. https://doi.org/10.1007/s00382-012-1644-1.
Knutti, Reto, Sedlacek, Jan, 2012. Robustness and uncertainties in the new CMIP5 climate model projections. Nat. Clim. Change. 3. https://doi.org/10.1038/nclimate1716.
Lanzante, John, Dixon, Keith, Nath, M., Whitlock, Carolyn, Adams-Smith, Dennis, 2017. Some pitfalls in statistical downscaling of future climate. Bull. Am. Meteorol. Soc. 99. https://doi.org/10.1175/BAMS-D-17-0046.1.
Lehner, Flavio, Wood, A., Vano, Julie, Lawrence, David, Clark, Martyn, Mankin, Justin, 2019. The potential to reduce uncertainty in regional runoff projections from climate models. Nat. Clim. Change 9, 926–933. https://doi.org/10.1038/s41558-019-0639-x.
Li, Feng-Rui, Feng, Qi, Liu, J.L., Sun, Te-Sheng, Ren, Wei, Guan, Zhen-Huan, 2013. Effects of the conversion of native vegetation to farmlands on soil microarthropod biodiversity and ecosystem functioning in a desert Oasis. Ecosystems 16. https://doi.org/10.1007/s10021-013-9689-5.
Lutz, Arthur, Immerzeel, W.W., Gobiet, Andreas, Pellicciotti, Francesca, Bierkens, M.F.P., 2013. Comparison of climate change signals in CMIP3 and CMIP5 multi-model ensembles and implications for central asian glaciers. Hydrol. Earth Syst. Sci. 17, 3661–3677. https://doi.org/10.5194/hess-17-3661-2013.
Mahmood, R., Mukand, Babel, 2012. Evaluation of SDSM developed by annual and monthly sub-models for downscaling temperature and precipitation in the jhelum basin, Pakistan and India. Theor. Appl. Climatol. 1–18.
Maury, Olivier, Campling, Liam, Arrizabalaga, Haritz, Aumont, Olivier, Bopp, Laurent, Merino, G., Squires, Dale, Cheung, William, Goujon, M., Guivarch, Céline, Lefort, Stelly, Marsac, Francis, Monteagudo, P., Murtugudde, Raghu, Österblom, Henrik, Pulvenis, J.F., Ye, Yimin, van Ruijven, Bas, 2017. From shared socio-economic pathways (SSPs) to oceanic system pathways (OSPs): building policy-relevant scenarios for global oceanic ecosystems and fisheries. Glob. Environ. Change 45, 203–216. https://doi.org/10.1016/j.gloenvcha.2017.06.007.
Miyan, M. Alimullah, 2015. Droughts in asian least developed countries: vulnerability and sustainability. SI: IGBP APN 7, 8–23. https://doi.org/10.1016/j.wace.2014.06.003.

Moore, Scott, 2011. Parchedness, politics, and power: the state hydraulic in Yemen. J. polit. ecol. 18. https://doi.org/10.2458/v18i1.21705.
Muharram, Ismail, Alsharjabi, Khalil, 2019. Sustainable Agriculture, Food Security and the Role of Agricultural Research and Technology Transfer in Yemen, pp. 441–462.
Onol, Baris, 2012. Effects of coastal topography on climate: high-resolution simulation with a regional climate model. Clim. Res. 52, 159–174. https://doi.org/10.3354/cr01077.
Ozturk, Tugba, Saygili-Araci, F.S., Kurnaz, M.L., 2021. Projected changes in extreme temperature and precipitation indices over CORDEX-MENA domain. Atmosphere 12 (5). https://doi.org/10.3390/atmos12050622.
O'Neill, Brian, Kriegler, Elmar, Ebi, Kristie, Kemp-Benedict, Eric, Riahi, Keywan, Rothman, Dale, van Ruijven, Bas, Vuuren, Detlef, Birkmann, Joern, Kok, Kasper, Levy, Marc, Solecki, William, 2015. The roads ahead: narratives for shared socioeconomic pathways describing world futures in the 21st century. Glob. Environ. Change 42. https://doi.org/10.1016/j.gloenvcha.2015.01.004.
Pietsch, Dana, Mabit, Lionel, 2012. Terrace soils in the Yemen highlands: using physical, chemical and radiometric data to assess their suitability for agriculture and their vulnerability to degradation. Geoderma 185–186, 48–60. https://doi.org/10.1016/j.geoderma.2012.03.027.
Poschlod, Benjamin, 2021. Using High-Resolution Regional Climate Models to Estimate Return Levels of Daily Extreme Precipitation over Bavaria.
Racherla, P., Shindell, D., Faluvegi, Gregory, 2012. The added value to global model projections of climate change by dynamical downscaling: a case study over the continental U.S. Using the GISS-ModelE2 and wrf models. J. Geophys. Res. 117, 20118. https://doi.org/10.1029/2012JD018091.
Rahman, Muhammad, Islam, Md, Jones, P., Hussain, Athar, Ashfaqur, 2012. Recent climate change in the arabian peninsula: seasonal rainfall and temperature climatology of Saudi Arabia for 1979-2009. Atmos. Res. 111, 29–45. https://doi.org/10.1016/j.atmosres.2012.02.013.
Rama, H.O., Roberts, Debra, Tignor, M., Poloczanska, E.S., Mintenbeck, Katja, Alegría, A., Craig, Marlies, Langsdorf, S., Löschke, S., Möller, Vincent, Okem, Andrew, Rama, B., Sina, Ayanlade, 2022. Climate Change 2022: Impacts, Adaptation and Vulnerability Working Group II Contribution to the Sixth Assessment Report of the. Intergovernmental Panel on Climate Change.
Rashid, Md Mamunur, Beecham, Simon, Chowdhury, Rezaul, 2014. Selection of Predictors for Statistical Downscaling Using Wavelet Techniques.
Refsgaard, Jens, Arnbjerg-Nielsen, Karsten, Drews, Martin, Halsnæs, Kirsten, Jeppesen, Erik, Madsen, Henrik, Markandya, Anil, Olesen, Jørgen, Porter, John, Christensen, Jens, 2013. The role of uncertainty in climate change adaptation strategies—a Danish water management example. Mitig. Adapt. Strategies Glob. Change 1–23. https://doi.org/10.1007/s11027-012-9366-6.
Riahi, Keywan, Vuuren, Detlef, Kriegler, Elmar, Edmonds, Jae, O'Neill, Brian, Fujimori, Shinichiro, Bauer, Nico, Calvin, Katherine, Dellink, Rob, Fricko, Oliver, Lutz, Wolfgang, Popp, Alexander, Cuaresma, Jesus Crespo, Samir, Kc, Leimbach, Marian, Jiang, Leiwen, Kram, Tom, Rao, Shilpa, Emmerling, Johannes, Tavoni, Massimo, 2016. The shared socioeconomic pathways and their energy, land use, and greenhouse gas emissions implications: an overview. Glob. Environ. Change 42. https://doi.org/10.1016/j.gloenvcha.2016.05.009.
Rosenblum, Erica, Eisenman, Ian, 2017. Sea ice trends in climate models only accurate in runs with biased global warming. J. Clim. 30. https://doi.org/10.1175/JCLI-D-16-0455.1.
Ruijs, A., de Bel, Mark, Kononen, Minna, Vincent, Linderhof, Nico, Polman, 2011. Adapting to Climate Variability: Learning from Past Experience and the Role of Institutions.
Sachindra, D.A., Huang, F., Barton, Andrew, Perera, B., 2012. Issues Associated with Statistical Downscaling of General Circulation Model Outputs: A Discussion.
Saddique, Naeem, Usman, Muhammad, Bernhofer, Christian, 2019a. Simulating the impact of climate change on the hydrological regimes of a sparsely gauged mountainous basin, northern Pakistan. Water 11. https://doi.org/10.3390/w11102141.
Saddique, Naeem, Usman, Muhammad, Bernhofer, Christian, Kronenberg, Rico, 2019b. Downscaling of CMIP5 models output by using statistical models in a data scarce mountain environment (mangla dam watershed), northern Pakistan. Asia Pac. J. Atmos. Sci. 55. https://doi.org/10.1007/s13143-019-00111-2.
Sanderson, Benjamin, O'Neill, Brian, Tebaldi, Claudia, 2016. What would it take to achieve the Paris temperature targets?: achieving the Paris temperature targets. Geophys. Res. Lett. 43. https://doi.org/10.1002/2016GL069563.
Sennikovs, Juris, Bethers, U., 2009. Statistical Downscaling Method of Regional Climate Model Results for Hydrological Modelling.
Souvignet, Maxime, Gaese, Hartmut, Ribbe, Lars, Kretschmer, Nicole, Oyarzun, Ricardo, 2010. Statistical downscaling of precipitation and temperature in north-Central Chile: an assessment of possible climate change impacts in an arid andean watershed. Hydrol. Sci. J. 55, 41–57. https://doi.org/10.1080/02626660903526045.
Swart, N.C., Cole, J.N.S., Kharin, V.V., Lazare, M., Scinocca, J.F., Gillett, N.P., Anstey, J., Arora, V., Christian, J.R., Hanna, S., Jiao, Y., Lee, W.G., Majaess, F., Saenko, O.A., Seiler, C., Seinen, C., Shao, A., Sigmond, M., Solheim, L., von Salzen, K., Yang, D., Winter, B., 2019. The Canadian Earth system model version 5 (CanESM5.0.3). Geosci. Model Dev. (GMD) 12 (11), 4823–4873. https://doi.org/10.5194/gmd-12-4823-2019.
Tahir, Tariq, Hashim, A., Yusof, Khamaruzaman Wan, 2018. Statistical downscaling of rainfall under transitional climate in limbang river basin by using SDSM. IOP Conf. Ser. Earth Environ. Sci. 140, 012037. https://doi.org/10.1088/1755-1315/140/1/012037.
Tavakol-Davani, Hassan, Nasseri, Mohsen, Zahraie, Banafsheh, 2013. Improved statistical downscaling of daily precipitation using SDSM platform and data-mining methods. Int. J. Climatol. 33. https://doi.org/10.1002/joc.3611.
Thompson, J., Green, A.J., Kingston, Daniel, Simon, Gosling, 2013. Assessment of uncertainty in river flow projections for the mekong river using multiple GCMs and hydrological models. J. Hydrol. 486, 1–30. https://doi.org/10.1016/j.jhydrol.2013.01.029.
Trzaska, Sylwia, Schnarr, Emilie, 2014. A Review of Downscaling Methods for Climate Change Projections.
Trzaska, Sylwia, Schnarr, Emilie, 2014a. A Review of Downscaling Methods for Climate Change Projections.
Tsegaw, Aynalem, Pontoppidan, Marie, Kristvik, Erle, Alfredsen, Knut, Muthanna, Tone, 2020. Hydrological impacts of climate change on small ungauged catchments -results from a global climate model-regional climate model-hydrologic model chain. Nat. Hazards Earth Syst. Sci. 20, 2133–2155. https://doi.org/10.5194/nhess-20-2133-2020.
van der Gun, Jac, Ahmed, Abdul, 1995. The Water Resources of Yemen. A Summary and Digest of Available Information (Text).
Varisco, Daniel, 1991. The future of terrace farming in Yemen: a development dilemma. Agric. Human Values 8, 166–172. https://doi.org/10.1007/BF01579671.
Varisco, Daniel, 2018. Agriculture in the northern highlands of Yemen: from subsistence to cash cropping. J. Arab. Stud. 8, 171–192. https://doi.org/10.1080/21534764.2018.1551470.
Varotsos, K., Karali, Anna, Lemesios, Giannis, Kitsara, Gianna, Moriondo, Marco, Dibari, Camilla, Leolini, Luisa, Giannakopoulos, Christos, 2021. Near future climate change projections with implications for the agricultural sector of three major mediterranean islands. Reg. Environ. Change 21. https://doi.org/10.1007/s10113-020-01736-0.
Vuuren, Detlef, Stehfest, E., Elzen, Michel, Kram, Tom, Vliet, Jasper, Deetman, Sebastiaan, Isaac, Morna, Goldewijk, Kees Klein, Hof, Andries, Beltran, Angelica Mendoza, Oostenrijk, Rineke, Ruijven, Bas van, 2011. RCP2.6: exploring the possibility to keep global mean temperature increase below 2°C. Clim. Change 109, 95–116. https://doi.org/10.1007/s10584-011-0152-3.
Wang, Dong, Liu, Jiahong, Shao, Weiwei, Mei, Chao, Su, Xin, Wang, Hao, 2021. Comparison of CMIP5 and CMIP6 multi-model ensemble for precipitation downscaling results and observational data: the case of hanjiang river basin. Atmosphere 12 (7). https://doi.org/10.3390/atmos12070867.
Ward, Ahmed, Wan, Ruslan Ismail, 2020. "Precipitation analysis and water resource of wadi siham basin. Yemen 7, 36–63.
Wiebelt, Manfred, Breisinger, Clemens, Ecker, Olivier, Al-Riffai, Perrihan, Robertson, Richard, Thiele, Rainer, 2011. Climate Change and Floods in Yemen: Impacts on Food Security and Options for Adaptation, vol. 1139.
Wilby, R.L., Dawson, C.W., 2007. SDSM 4.2-A Decision Support Tool for the Assessment of Regional Climate Change Impacts. Lancaster University, Lancaster/Environment Agency of England and Wales, Lancaster, Lancaster, England.
Wilby, R.L., Dawson, C.W., 2013. The statistical DownScaling model: insights from one decade of application. Int. J. Climatol. 33 (7), 1707–1719. https://doi.org/10.1002/joc.3544.
Wilby, Robert, Yu, Dapeng, 2013. Mapping Climate Change Impacts on Smallholder Agriculture in Yemen Using GIS Modelling Approaches.
Wilby, Robert, Dawson, C., Barrow, E.M., 2002. Sdsm – a decision support tool for the assessment of regional climate change impacts. Environ. Model. Software 17, 145–157. https://doi.org/10.1016/S1364-8152(01)00060-3.
Wilby, R.L., Troni, J., Biot, Y., Tedd, L., Hewitson, B.C., Smith, D.M., Sutton, R.T., 2009. A review of climate risk information for adaptation and development planning. Int. J. Climatol. 29 (9), 1193–1215. https://doi.org/10.1002/joc.1839.
Wilby, Robert, Dawson, C., Murphy, Conor, O'Connor, Paul, Hawkins, Ed, 2014. The statistical DownScaling model -decision centric (SDSM-DC): conceptual basis and applications. Clim. Res. 61. https://doi.org/10.3354/cr01254.
Winton, M., Adcroft, Alistair, Dunne, J., Held, Isaac, Shevliakova, Elena, Zhao, M., Guo, H., Hurlin, W., Krasting, J., Knutson, T., Paynter, D., Silvers, Levi, Zhang, R., 2020. Climate sensitivity of GFDL's CM4.0. J. Adv. Model. Earth Syst. 12. https://doi.org/10.1029/2019MS001838.
Yazdandoost, Farhad, Moradian, Sogol, Izadi, Ardalan, Aghakouchak, Amir, 2020. Evaluation of CMIP6 precipitation simulations across different climatic zones: uncertainty and model Intercomparison. Atmos. Res. 250. https://doi.org/10.1016/j.atmosres.2020.105369.
Ye, Hengchun, 2018. Changes in duration of dry and wet spells associated with air temperatures in Russia. Environ. Res. Lett. 13 (3), 034036. https://doi.org/10.1088/1748-9326/aaae0d.
Zeleňáková, Martina, Abd-Elhamid, Hany F., Krajníková, Katarína, Smetanková, Jana, Purcz, Pavol, Alkhalaf, Ibrahim, 2022. Spatial and temporal variability of rainfall trends in response to climate change—a case study: Syria. Water 14 (10). https://doi.org/10.3390/w14101670.
Zhang, Lei, Xu, YinLong, Meng, Chunchun, Li, XinHua, Liu, Huan, Wang, ChangGui, 2019. Comparison of statistical and dynamic downscaling techniques in generating high-resolution temperatures in China from CMIP5 GCMs. J. Appl. Meteorol. Climatol. 59. https://doi.org/10.1175/JAMC-D-19-0048.1.